Role of Caveolin-1 in Hypoxia and Proneural to Mesenchymal Transition of Glioblastoma

Somdutta Kundu

This thesis is submitted in partial fulfilment of the requirements for the degree of Master in Biomedical Sciences

Department of Biomedicine

University of Bergen

Spring Semester 2018

Acknowledgements

This work was carried out in the period of August 2017 to May 2018 at the Department of Biomedicine, University of Bergen, Norway. Firstly, I would like to express my sincerest gratitude to my supervisor Prof. Dr. Hrvoje Miletic for giving me this opportunity to work in this interesting project. I am gratefully indebted for his cordial supervision and inspiration to bring the best out of me. I was blessed with his valuable suggestions that made this project possible within the limited time frame. I would like to thank Prof. Dr. Rolf Bjerkvig for providing the infrastructure of K.G. Jebsen Brain Tumour Research Centre.

I would like to thank my co-supervisor Dr. Justin Joseph for his guidance and time throughout the thesis. Cordial thanks to my lab fellows Mohummad Aminur Rahman, Md Abdul latif and Jubayer Hossain for continuous help, inspiration, and kind co-operation during the period of project work.

Great thanks to Dr. Rolf Bjerkvig, Dr. Hrvoje Miletic, Dr. Martha Chekenya Enger, Dr. Marit Bakke, Dr. Frits Alan Thorsen, Dr. Stein Ove Døskeland, Dr. Elon Donald Gullberg, and all of my respective faculty members for delivering lectures, which helps me in the thesis, during the study period.

Special thanks to my research group, Translational Cancer Research Group for creating a friendly and energetic atmosphere. Thanks to Sandra for her great support in my entire project, especially in cell culture lab and also for some scientific discussions.

The help from technical engineers: Halala, Marzieh, Romi and Tuyen is much appreciated. I am thankful to my project fellow Frida Haukås for helping me lot in my project initially. My deepest respect to my parents and in-laws for their support and encouragement in all of my pursuits. Last but not least, to my husband for his perseverance and unconditional support in my well and woe.

Finally, to all my fellow students – the last two years have been GREAT!

Somdutta Kundu

Bergen, 2018

Table of contents

List of figures

List of tables

List of abbreviations

ARNT	Aryl hydrocarbon receptor nuclear translocator
BBB	Blood brain barrier
BSA	Bovine serum albumin
Cav-1	Caveolin-1
CBP	CREB-binding protein
CLS	Classical subtypes
CNS	Central nervous system
CREB	cAMP response element binding
CSC	Cancer stem cell
CSD	Cav-1 scaffolding domain
DAPI	4′,6-diamidino-2-phenylindole
DMSO	Dimethyl Sulfoxide
DNA	Deoxyribo nucleic acid
ECM	Extracellular matrix
EGFR	Epidermal growth factor receptor
EHS	Engelbreth-Holm-Swarm (EHS) mouse sarcoma
EMT	Epithelial- mesenchymal transition
eNOS	endothelial nitric oxide synthase
ER	Endoplasmatic reticulum
GAPDH	Glyceraldehyde-3-phosphate dehydrogenase
GBM	Glioblastoma multiforme
GSC	Glioblastoma stem-like cell

HCMV	Human Cytomegalovirus
HGF	Hepatocyte growth factor receptor
HIF-1α	Hypoxia inducible factor- 1α
HRE	Hypoxia response element
HRP	Horseradish peroxidase
ICC	Immunocytochemistry
IDH1	Isocitrate dehydrogenase 1
IHC	Immunohistochemistry
LFS	Li–Fraumeni syndrome
LOH	Loss of Heterozygosity
MAPK	Mitogen-activated protein kinase
MDM2	Mouse double minute 2 homolog
MES	Mesenchymal subtypes
MGES	Mesenchymal gene expression signature
MOPS	3-(N-morpholine)-propane sulphonic acid (buffer)
MRI	Magnetic resonance imaging
mTOR	Mammalian target of rapamycin
NBM	Neurobasal medium
NF1	Neurofibromatosis type-1
NF2	Neurofibromatosis type-2
nM	Nanomolar
PDGFR	Platelets Derived Growth Factor Receptor
PFA	Paraformaldehyde
PHD	Prolyl hydroxylase domain

PI3K	Phosphatidylinositol-4,5-bisphosphate 3-kinase
PNS	Proneural subtypes
PNGES	Proneural gene expression signature
PTEN	Phosphatase and tensin homologue
pVHL	Polyubiquitinated von Hippel–Lindau
RB	Retinoblastoma
rpm	Revolutions per minute
RTK	Receptor tyrosine kinase
SDS-PAGE	Sodium dodecyl sulfate polyacrylamide gel electrophoresis
STAT3	Signal transducer and activator of transcription 3
TBST	Tris-buffered saline with Tween-20
TCGA	The Cancer Genome Atlas
TGF- β	Transforming growth factor-β
TME	Tumor microenvironment
TP53	Tumor protein 53
V	Volt
VEGF	Vascular endothelial growth factor
VHL	Von Hippel Lindau disease
v/v	Volume/ volume
w/v	Weight/ volume
WHO	World Health Organization
^{o}C	degree Celsius

Summary

Glioblastomas (GBM), a grade IV astrocytoma, is the most common and aggressive primary brain tumors in adults, associated with short survival and uniformly fatal outcome irrespective of treatment. GBM is highly heterogeneous at both molecular and histological levels, including pseudopalisading necrosis, that make GBM most hypoxic and angiogenic tumor in nature. Recent transcriptomic profiling has identified 4 distinct subtypes of GBM based on specific gene expression pattern. Of these the mesenchymal GBM subtype was reported to be the most aggressive one with the worst clinical outcome. Caveolin-1 (Cav-1) is well known principle scaffolding protein in caveole that directly interacts with several signalling molecules and play crucial role in numerous signalling pathways. Over the past 10-15 years, Cav-1 has been found to have oncogenic and metastasis promoting roles in many aspects depending on the tumour type or tissue of interest.

Within our project we investigated the role of a hypoxic microenvironment on Cav-1 expression and on mesenchymal and proneural markers by western blotting. Our preliminary data indicate that Cav-1 is elevated under hypoxia in a fraction of GBM cell lines. Upregulation of Cav-1 was confirmed in GBM patient samples around necrotic areas, however, expression pattern of Cav-1 showed inter- and intra-tumoral heterogeneity. Despite the heterogeneity, Cav-1 expression was found to be highly upregulated in hypoxic regions in most of GBM samples, indicating a possible connection between hypoxia and Cav-1 expression. TCGA patient data indicated a correlation of Cav-1 with mesenchymal markers and anti-correlation with proneural markers. Thus, we further investigated whether hypoxia induced a proneural to mesenchymal switch in GBM cell lines. Proneural markers PDGFRA and olig2 were downregulated under hypoxia, however no clear pattern for the mesenchymal markers YKL40, pSTAT3 and CD44 was observed.

In conclusion, our results show that Cav-1 is upregulated under hypoxia in a subset of GBM, which parallels downregulation of proneural markers. Whether a mesenchymal shift is induced under hypoxia and whether this might be dependent on Cav-1 needs to be elucidated in future studies.

1. Introduction

1.1 Cancer

Cancer is a group of diseases that can affect most organs of the body and is caused by mutations in the genome of normal cells. Cancer development is a multistep process caused by successive changes, such as a series of genetic mutations in the DNA of one cell, inhibition of cell differentiation and avoidance of cell death. The cancer cells are able to invade into surrounding tissue, metastasize and finally kill the host as the result of an expansive disease affecting multiple organs.[1,2] Cancer is one of the most frequent global causes of death.[3] Despite significant research to understand the mechanism of cancer development during the last decades, the basic mechanism for tumour initiation and progression has not yet been fully understood. It is estimated that approximately 21.4 million people suffer from cancer and most of them will likely die of it.[4] Thus, despite a lot of money and human efforts spent on research in the last decades, cancer still remains a major cause of death and an economic burden. Thus, research aimed at developing novel effective treatments is of utmost importance.

1.2 Development of cancer

The accumulation of mutations in the genes that directly control cell division or cell death causes the cancer, but the actual mechanism, how these mutations are generated, is still under debate. It has also been suggested that normal rates of mutation, together with waves of clonal expansion, are enough to facilitate the process in humans. Genetic modifications such as distinct sequence changes, invariable alterations in chromosome numbers, translocation of chromosomes and gene amplifications affect growth-controlling genes in neoplastic cells.[5]

The well-known concept of the six hallmarks of cancer, introduced by Hanahan and Weinberg in 2000, contains six biological capabilities acquired during the multistep development of human tumours.[6] During the remarkable progress in cancer research, these hallmarks constitute an organizing principle for rationalizing the complexities of neoplastic disease that includes:

1) The ability to sustain chronic proliferation and release of growth promoting signals;

2) Evading growth suppressors;

3) Resistance to programmed cell death;

4) Ability to form new blood vessels by angiogenesis;

5) Enduring replicative potential;

6) Generate secondary tumours at distant sites by metastasis as well as invasion or invasion-metastasis cascade.[6]

Recently these hallmarks were extended by the same authors to include reprogramming of energy metabolism as both direct and indirect consequence of oncogenic mutations and the ability to avoid immune destruction.[7]

In general, there are two types of mutations that lead to cancer development. Oncogenic mutations are gain of function mutations and induce either overexpression of the gene or over-activation of the related protein. An oncogene may either encode for a growth factor or a component within a mitotic signalling cascade inside the cell. Oncogenic mutations are dominant, that means that only one allele needs to become mutated in order to influence cancer development. The second type of mutations are loss of function mutations in tumor suppressor genes. These genes encode for proteins that inhibit cell cycle progression or promote apoptosis in case of deleterious stress to the cell.[8] A well-known tumour suppressor gene is p53, which is mutated in over 50 % of all cancers and induces apoptosis in case of irreparably damaged DNA.[9] Both alleles of a tumour suppressor gene have to become mutated in order to influence cancer development, hence mutations in tumour suppressor genes are recessive mutations. There are two main consequences of activated oncogenes or inactivated tumour suppressor genes such as:

1) the proofreading machinery that normally prevents a damaged cell from dividing is not working or the signalling pathways mediating programmed cell death are disrupted.

2) the cell achieves stronger mitotic signals and divides faster. This leads to increasing genomic instability, additional mutations and uncontrolled development of an abnormal cell mass.

Cancer cells also release various signalling molecules with a broad range of biological effects on the microenvironment, including remodelling of the extracellular matrix and induction tumour vasculature termed angiogenesis. These effects lead to spread of tumor cells from the primary site to distant organs, a process which is termed metastasis. Most cancer related deaths result from metastatic spread. The metastatic process starts with migration of cancer cells from the primary site to a blood vessel, where the cells intravasate into the blood circulation. Cells are transported with the blood flow and eventually invade into another organ, a process which is still poorly understood. The whole process of metastasis depends on a range of factors, including the ability to evade immune destruction, altered expression of cell adhesion molecules, as well as activation of enzymes that break down the extracellular constituents that restrain cells to one place. Moreover, when the metastasizing cancer cells reach their final destination, the microenvironment must be permissive to sustain growth of the cancer cells.[10] A recent review by Ribatti et al. summarizes the current knowledge on the spreading of certain cancers to specific organs.[11]

1.3 Overview of brain cancers

The brain and spinal cord together form the central nervous system (CNS) which is essential for our existence. Cancers of the central nervous system (CNS) are classified based on their similarity to the main cell types of the CNS. A major portion of CNS malignancies (gliomas, around 81%) arise from "glia" which are the supportive tissue of the brain.[12] Even though primary brain tumours constitute only 2% of all cancer cases,[13] their dismal prognosis makes it an important research focus. According to the World Health Organization (WHO), primary brain tumors are classified as ependymoma, astrocytoma and oliogodendroglioma and.[13] Astrocytomas represent a major proportion (approximately 75%) of all gliomas. Amongst these, glioblastoma accounts for 55% and is the most aggressive in adults.[14]The WHO has further subclassified astrocytomas into four grades of malignancy (Grade I, II, III and IV) depending on specific histological criteria.[13] Histological grading considers the presence of nuclear atypia, mitotic activity, microvascular proliferation and necroses. The classification of astrocytomas is summarized in table 1. WHO Grade I pilocytic astrocytoma is a benign, circumscribed tumour without nuclear atypia and no visible mitotic activity and most often occurs in children. It has a good prognosis and mostly requires surgical resection only. WHO

grade II-IV tumors Grade II (fibrillary astrocytoma) is characterized by moderate nuclear atypia and diffuse invasion into the brain parenchyma. Anaplastic astrocytomas (grade III) are also highly invasive and show in addition high nuclear atypia and mitotic activity. Glioblastoma is categorized as WHO grade IV and is differentiated from anaplastic astrocytoma by the presence of microvascular proliferations and necrotic areas. The histological grading strongly correlates with clinical outcome.[15] Low-grade gliomas are clinically less aggressive, and exhibit better overall survival outcome compared to high-grade gliomas.

Table 1. WHO classification and grading of astrocytomas

Grade	Designation	Histological feature
I.	Pilocytic astrocytoma	benign, without nuclear atypia
II.	Astrocytoma (low-grade, diffuse)	Moderate nuclear atypia
III.	Anaplastic astrocytoma	High nuclear atypia and mitotic activity
IV.	Glioblastoma	High nuclear atypia, mitotic activity, microvascular proliferation and necrosis

1.4 Glioblastoma

Glioblastoma (GBM) is the most frequent and most aggressive primary intracranial brain malignancy in adults.[16, 17] GBM most likely arises from astrocytes or its precursor cells, which are important supportive glial cells in the brain. Patients with GBM have a poor prognosis with a median survival time less than 16 months.[18] Percival Bailey and Harvey Cushing revealed the term almost a century ago due to resemblance of predominant progenitor (blast) cells of embryonic nervous system (Glioblastoma). The term multiforme was used to describe GBMs´characteristic intra- and inter-tumoural heterogeneity.[19]

The incidence of GBM increases with age, mainly after 58 years. About 8.8% of children with central nervous system tumours have GBM[20] and congenital cases are rare. GBM occurs more

often in men than woman with a ratio of 3:2 and the reason for this gender distribution is still unknown.[21] GBM usually appear sporadically, but several genetic disorders are associated with increased incidence including neurofibromatosis type-1 (NF1) and type-2 (NF2), Li–Fraumeni syndrome (LFS), Von Hippel Lindau disease (VHL),[21] tuberous sclerosis, Turcot syndrome and multiple endocrine neoplasia type IIA. In addition, acquired head injuries, which occurred as a result of a brain contusion, may predispose to the onset of glioblastoma.[22, 23]

It was believed that viruses, such as human cytomegalovirus (HCMV), causes glioma development and stimulates congenital encephalitis and multi-organ changes in adults. Human cytomegalovirus displays tropism for glial cells. Since the viral genes encode proteins (e.g. IE1, US28, GB), they activate intracellular signalling pathways involved in mitogenesis, mutagenesis, apoptosis, inflammation and angiogenesis. Thus, products of these genes cause disruption of the key signalling pathways (including PDGFR, Akt, STAT3), but also cause troubles in monocyte and glial cell functions.[24, 25]

Ionizing radiation is one of causes for developing this type of tumour. Chemicals like pesticides, polycyclic aromatic compounds and solvents are also considered as potentially dangerous. At the same time, electromagnetic fields and certain metals cause glioma development.[26] Although the use of a mobile phone does not increase the risk of developing glioblastoma, the long-term effect for using of mobile phones is still not clear. Moreover, working peoples in the rubber and petrochemical industry have higher risk for glioma development. Thus, glioblastoma is considered as an occupational disease.[27, 28]

GBM cells generally show rapid cell proliferation and induce pathologic tumor vascularization which produces tumour areas with insufficient oxygen supply.[29] This chronic exposure to extremely low levels of oxygen frequently produces necrotic zones surrounded by densely packed hypoxic tumour cells. These so-called pseudo-palisading GBM cells were shown to express hypoxia-regulated genes that control crucial processes associated with tumour aggressiveness such as angiogenesis, extracellular matrix degradation, and invasive behaviour.[30, 31] Hypoxia is also a well-recognized component of the tumour microenvironment and has been linked to poor patient outcome and resistance to therapies in different cancer types.[32]

1.4.1 Classification of GBM

GBM is classified as either primary or secondary in origin. Primary GBM (de novo) arises from normal glial cells or its progenitor cells in around 90% of diagnosed GBM cases without prior evidence of less malignant lesions. The remaining 10% GBM cases are secondary lesions originating from low-grade or anaplastic astrocytoma. The transformation process from low grade to high grade astrocytoma and secondary GBM mostly takes several years.[33-35]

Primary and secondary GBM show no morphological differences. However, the genetic basis, as well as the molecular pathways involved in the development of primary and secondary GBMs are different (Fig. 1). Primary GBM are characterized by LOH chromosome 10q (69%), a high frequency of EGFR amplification (45%), p16 INK4a deletion, MDM2 amplification and loss of PTEN (24–34%). In contrast, secondary GBMs are characterized by IDH1 and P53 mutations, RB gene alterations, and amplification and/or overexpression of the PDGFR gene.[36] Common to both primary and secondary glioblastoma is LOH on 10q, which is distal to the PTEN locus. Of the TP53 point mutations in secondary glioblastomas, 57% are located in hotspot codons 248 and 273, while in primary glioblastomas, mutations are more widely distributed.[33] These genetic changes together with differences in the transcriptome define molecular subclasses of GBM which are mesenchymal, classical and proneural.[37, 38]

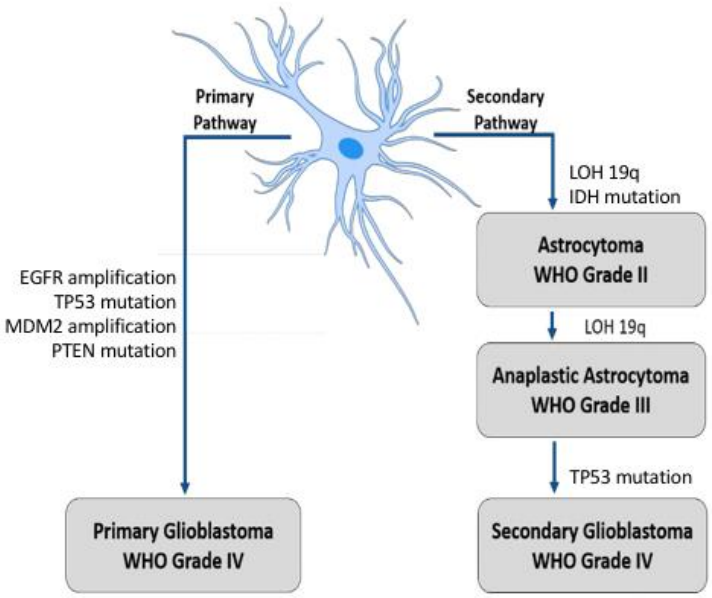

Fig. 1 Genetic alterations in primary and secondary glioma. (taken from[39])

1.4.2 Symptoms and diagnosis

Common clinical symptoms are dysphagia, seizures, headaches, cognitive changes, vision disturbance (blurred vision, diplopia), vomiting, ataxia, dizziness, and frequent syncopes.[40, 41] Due to these unspecific symptoms, gliomas can be misdiagnosed and therefore radiology is an important step in the diagnostic process.[42] Gliomas most frequently arise in the frontal lobes (40%), while temporal and parietal lobes account for 29% and 14% of cases, respectively.[43] Progression of high intracranial pressure is one of the most dangerous features of GBM.[40]

Imaging techniques such as magnetic resonance imaging or computer tomography is the primary diagnostic tool for GBM. Post contrast T1 weighted spin echo MRI images show irregular hypo-intense signal with ring like enhancement at the tumour margin which indicates disruption of blood brain barrier (BBB) in GBM.[44] This is also an indicator of neo-angiogenesis, the process whereby new vessels are formed by sprouting from pre-existing blood vessels. T2 diffusion weighted MRI is useful for evaluation of peri-tumour oedema that appears as a hyper-intense signal (Fig. 2). Cerebral abscess, vascular infarction, lymphoma or metastases from distant organ sites can mimic glioblastoma on neuroimaging, thus the final diagnosis is determined by histology.

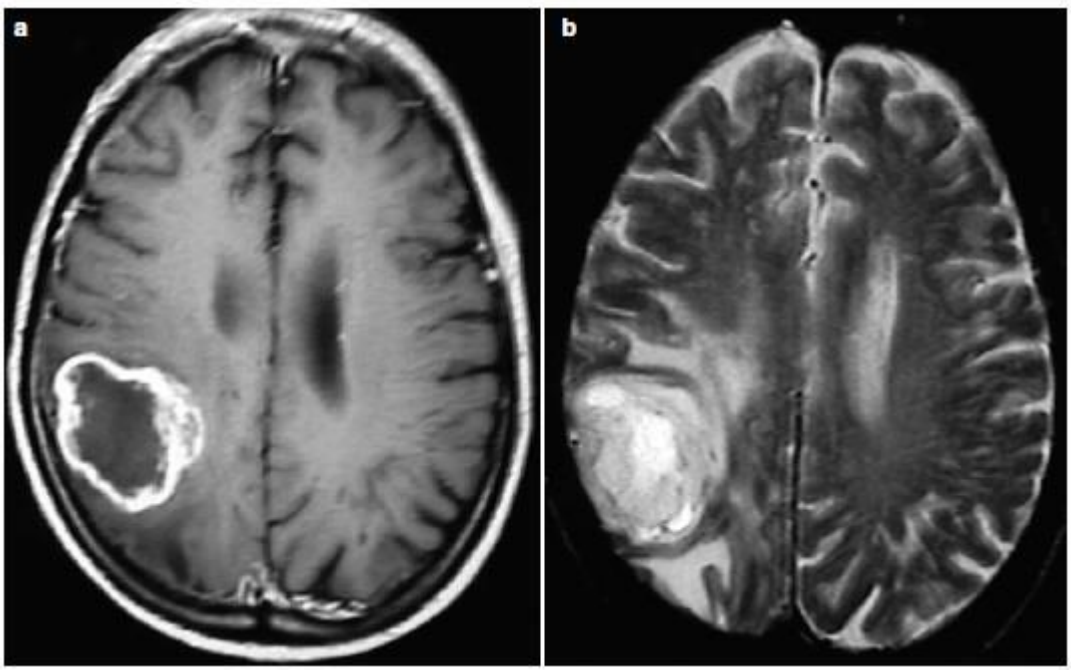

Fig. 2 Magnetic resonance imaging of Glioblastoma. GBM in right parietal lobe a) Post contrast T1-weighted image

shows irregular ring shaped enhanced signal b) T2 weighted image shows high signal intensity with oedema surrounding tumour. (taken from [44])

1.4.3 Macroscopic features

Macroscopically, GBM lesions vary in size, usually 5-10 cm in diameter in most of the cases.[27] Lesions usually present as intraparenchymal round masses where the borders between normal and pathological tissue are poorly demarcated (Fig. 3). Peritumoural oedema with mass effect contributes to shift of midline structures. Concurrent haemorrhage and or necrosis give a variegated appearance of the tumour. Tumours are mostly solitary, but can spread to the contralateral hemisphere and give rise to butterfly-like lesion. Uneven distribution and poor margin of the tumour is a huge obstacle for GBM surgery. Maximal resection with adjuvant therapy cannot prevent recurrence of the tumour.

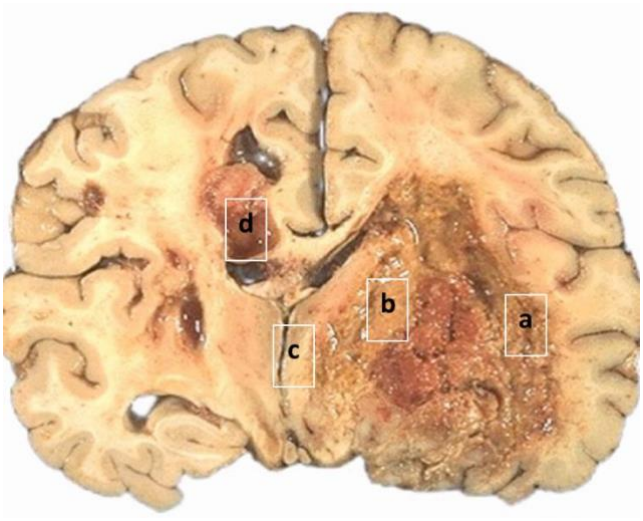

Fig. 3 Gross morphology of Glioblastoma. Coronal section of a Glioblastoma showing- a) irregular margin b) necrosis c) midline shifting d) contralateral hemorrhage. (taken from http://library.med.utah.edu/WebPath/CNSHTML/CNS136.html)

1.4.4 Microscopic feature

GBMs are hypercellular and extremely mitotically active tumors. This ends up in an extreme unmet demand for oxygenation and metabolism resulting in hypoxia and tissue necrosis. GBM has an important feature called Necrotic foci. There are two types of necrosis depending on the size and position of the necrotic area. First type has large areas of necrosis within the

main area of the tumour. This type appears due to inadequate blood supply in all primary glioblastomas. The other type can easily be detected by tiny, unevenly shaped necrotic foci encircled by pseudopalisading zone. This type appears in both primary and secondary glioblastomas (Fig. 4).[45] Pseudopalisades are typically 30 - 1500 μm in the internal width and 50 - 3500 μm in the internal length.[31]

Hypoxia in turn upregulates hypoxia-inducible factor 1-alpha (HIF-1α) leading to increased vascular endothelial growth factor (VEGF) secretion that induces sprouting of new blood vessels from the pre-existing through angiogenesis. GBM is thus highly vascularized by unique microvessels forming glomeruloid tufts lacking lumen and BBB. These microvascular proliferations are leaky and contribute to the development of edema. Moreover, the tumour cells invade diffusely into the brain parenchyma, which contributes to recurrence and treatment failure.[27]

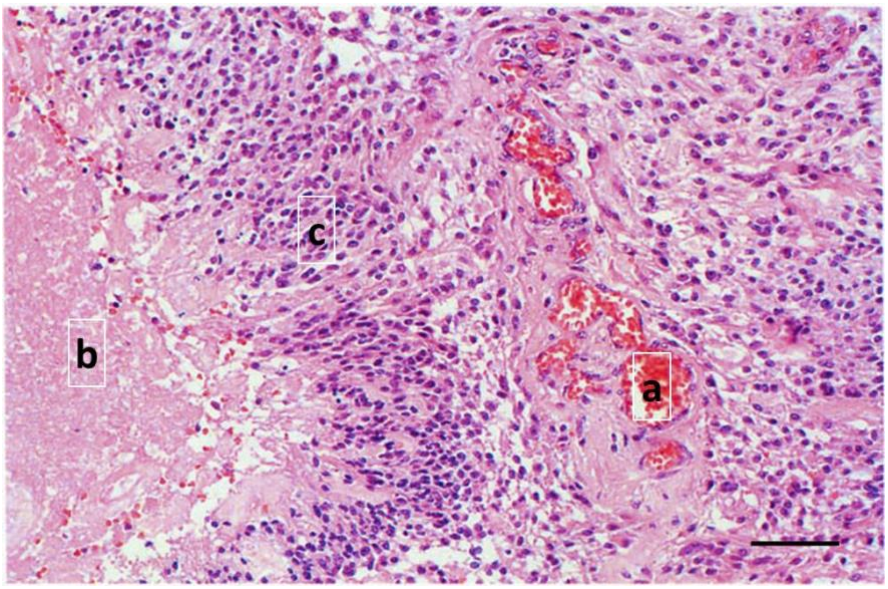

Fig. 4 Histological H&E staining of GBM showing a) Glomerular pattern of angiogenesis (microvascular proliferation), b) central area of necrosis c) arrangement of tumour cells surrounding necrosis-pseudopalisading necrosis. Magnification 100X, scale bar = 100 μm. (taken from [45])

1.5 Hypoxia and the role of hypoxia-inducible factors in GBM

In addition to the features described above, GBM show a high degree of infiltration of diverse immune cells, including microglia, macrophages, and lymphocytes.[46, 47] This composition

cells generate a GBM-specific tumour microenvironment (TME), which plays a crucial role in tumour progression, immune escape, local invasion and distant invasion of GBM.[48, 49] The tumour and its surrounding microenvironment are closely related and interact constantly.[50] During the stages of tumour progression, a hypoxic TME or pro-oxidant-enriched TME is formed; these TMEs have both beneficial and harmful effects on tumour cells and their niche. The TME is characterized by low levels of glucose and amino acids, acidosis, and hypoxia.[51]

A Hypoxic state arises in glioblastomas because of uncontrolled cell proliferation, erratic tumour neovascularization, poor oxygen diffusion, disruption of the blood-brain barrier, poor permeability of nitric oxide and intra-tumoral necrosis that interferes with oxygen perfusion (Fig. 5).[52] Tumour hypoxia is associated with metastases,[53] recurrences[54] and resistance to chemotherapy and radiation therapy.[55] These effects are mediated by a family of transcription factors called hypoxia-inducible factors (HIF-1α and HIF-2α).[56] HIF-1α expression and activity is highly dependent on oxygen supply; under normoxic conditions, HIF-1α is rapidly hydroxylated by prolyl hydroxylase domain (PHD)-containing proteins and subsequently polyubiquitinated by the von Hippel–Lindau tumour suppressor (pVHL) for degradation through the proteasome pathway.[56] Under hypoxic conditions, pVHL-mediated HIF-1α degradation is abolished, causing HIF-1α to accumulate and translocate to the nucleus where it forms a heterodimer with HIF-1β, which can bind to hypoxia responsive elements (HREs) in the promoters of hypoxia-regulated genes.[57, 58]

Furthermore, hypoxic areas detected in GBM can correlate with poorer outcomes and greater proliferation of CSCs, which may drive tumour resistance and recurrence, as well as regulation of the tumour microenvironment.[52]

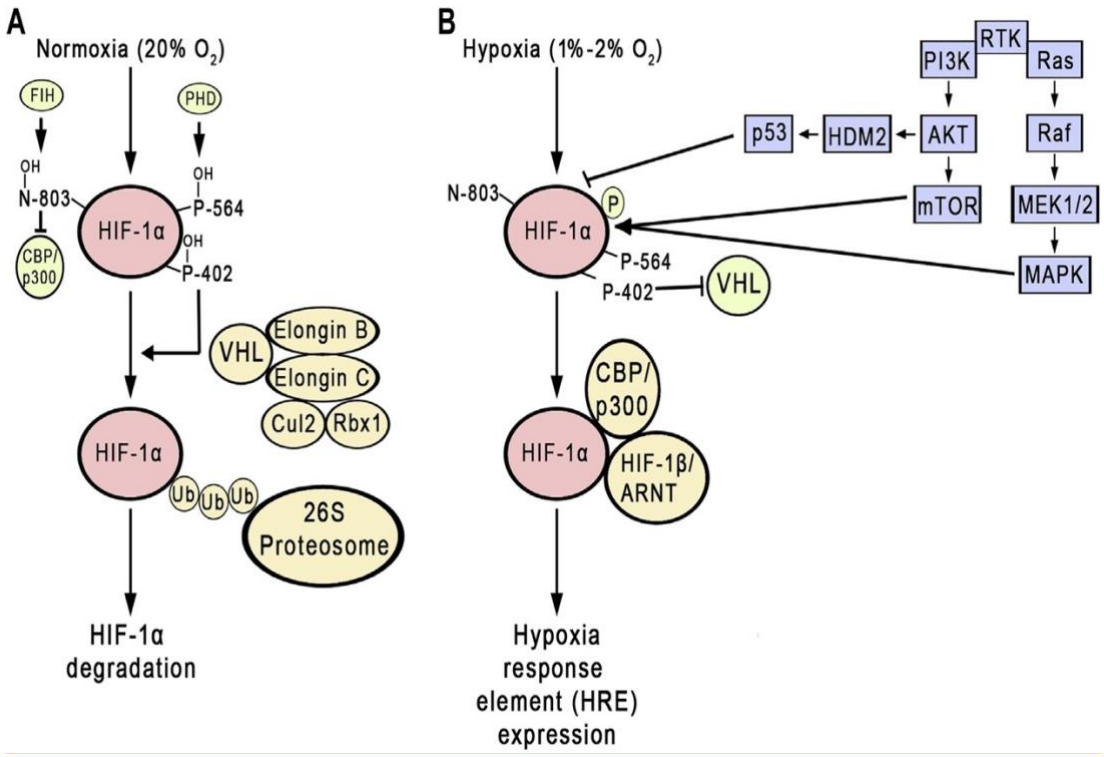

Fig. 5 Regulation of hypoxia signalling in glioblastoma. Hypoxia-inducible factor (HIF) signalling during normoxia and hypoxia as well as the interaction between HIFs and epithelial-mesenchymal transition are represented in glioblastoma. (A) During normoxia, increased activity of prolyl hydroxylase domain (PHD)-containing protein level that results in hydroxylation of HIF-1α residues (P-564, P-402), which recruits the von Hippel-Lindau (VHL) complex. (B) During hypoxia (1%-2% O_2), HIF-1α remains unhydroxylated, resulting in recruitment of HIF-1β/aryl hydrocarbon receptor nuclear translocator (ARNT) and the coactivator CBP/p300, which bind to hypoxia response elements (HRE) involving expression of several hundred downstream transcription factors, including those involved in mesenchymal transformation. HIF-1α can also be upregulated by various downstream regulators from receptor tyrosine kinases (e.g., PI3K/AKT/mTOR, Ras/Raf/MAPK). Cul2, cullin 2; MAPK, mitogen-activated protein kinase; MEK1/2, MAPK kinase; mTOR, mammalian target of rapamycin; PI3K, phosphatidylinositol-4,5-bisphosphate 3-kinase; Rbx1, ring-box 1, E3 ubiquitin protein ligase; RTK, receptor tyrosine kinase. (taken from [59])

An important downstream activation of HIF signalling cascade is angiogenesis. Not surprisingly, a histologic hallmark of glioblastoma is microvascular proliferation. Despite the apparent abundance of angiogenic activity, a characteristic feature of glioblastoma is abnormally functioning blood vessels. Vessels lack the structural support of pericytes and are characteristically tortuous and leaky, impeding blood flow and decreasing perfusion.[60] At the tumour tissue level, microvascular thromboses occlude vessels, further promoting intratumoral hypoxia.[60] Because the volume of blood flow influences regional tissue

oxygenation, understanding the crosstalk between GSCs and the neighbouring blood vessels may provide novel therapeutic opportunities.

1.6. Epithelial-mesenchymal transition (EMT)

Epithelial-mesenchymal transition (EMT) is a reversible biological process in which polarized epithelial cells are induced to undergo numerous biochemical changes including loss of epithelial cell polarity, loss of cell-cell contacts, and increased motility that results in a mesenchymal phenotype, characterized by an enhanced migratory capacity and elevated resistance to genotoxic agents (Fig. 6). Additionally, EMT is a vital inducer of the cancer stem cell phenotype. GBM is not an epitehelial cancer, however, an EMT-like process has been described for GBM. On this point, the mesenchymal subtype of glioblastoma (GBM) is associated with a destructive phenotype. The existence of a CSC population has also been proven in malignant gliomas, however, the co-existence of a stem cell status with EMT(-like) processes in GBMs has been described only recently.[61, 62]

The microenvironment that induces EMT in gliomas is characterized by hypoxia and the enrichment of myeloid cells following stimulation by transforming growth factor-β (TGF- β), epidermal growth factor, platelet-derived growth factor and fibroblast growth factor-2 and also numerous proteases that increase invasiveness into the surrounding normal brain.[63]

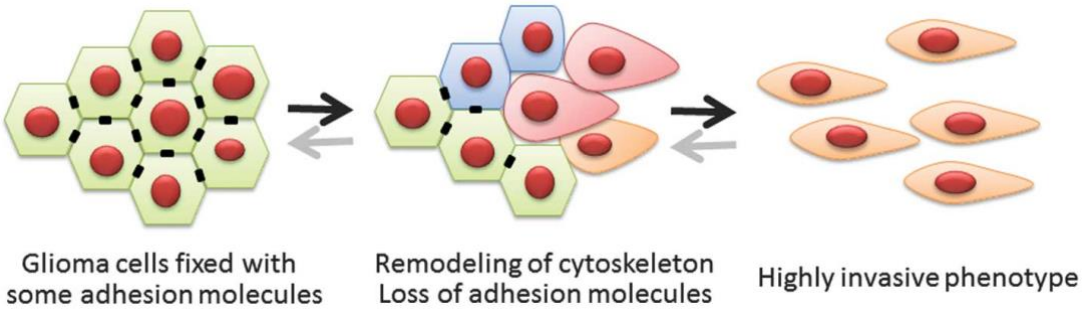

Fig. 6 Scheme for the epithelial-mesenchymal transition in glioma cells. (taken from [63])

1.7 Formation of Caveolae, Cavins, Caveolin-1 and its versatility

Caveolae are plasma membrane subdomains of distinct lipid and protein compositions present in many mammalian cells. These submicroscopic, flask-shaped invaginations, occupy up to 20% of the plasma membrane which play multiple roles in cell physiology, including

signalling platforms for numerous pathways, clathrin-independent routes of endocytosis, lipid homeostasis, tumorigenesis, mechano-transduction and mechanical stress sensors.[64, 65]

The formation of cholesterol-rich, small Ω- shaped caveolae require a protein family called caveolins, in which caveolin-1, best known as a membrane integral protein, is a key component of caveole structure. Caveolae were first morphologically identified in 1950s by transmission electron microscopy and were described as structures resembling `little caves' due to their appearance as 50- to 100-nm vesicular invaginations of the plasma membrane and Cav-1 or VIP21 was first identified in Rous sarcoma transfected cells and found to be a substrate of v-Src and trans-Golgi derived transport vesicles. Since then, three isoforms of the caveolin family, caveolin-1, -2, and -3 have been identified and all of them are sufficient for caveolae formation in most tissues and striated muscle, respectively. Cav-2 associates with Cav-1 in hetero-oligomers and does not independently form caveolae.[66] Additionally caveole formation and functions are known to involve a family of cytoplasmic proteins named cavins. Cavin-1 (polymerase I) and transcript release factor (PTRF), are only essential for caveolae formation. Additionally, it involves in transcription termination via interaction with RNA polymerase and in regulation of type I collagen gene expression by interacting with a DNA-binding transcription factor.[67, 68]

Caveolae are thought to function as signalling platforms regulating the activation of several signaling pathways such as many receptor and non-receptor tyrosine kinases, hepatocyte growth factor (HGF) receptor, platelet- derived growth factor receptor (PDGFR), epidermal growth factor receptor (EGFR), endothelial nitric oxide synthase (eNOS), proteins involved in calcium transport, H-Ras, integrins, nerve growth factor, serine/threonine kinases, phospholipases, G protein-coupled receptors and Src family kinases. Cav-1 binds and tonically inhibits the activation of such signalling platforms which facilitate the signaling cascades that contribute to cancer regulation. As a consequence, many studies recognize Cav-1 as a modulator of cell transformation, proliferation and metastasis.[69]

Cav-1 is well known principle scaffolding protein of caveole that directly interacts with several signalling molecules (growth factor receptors, kinases, G- proteins and adhesion molecules) in caveolae to control their subcellular distribution and activation status[70, 71] Human Cav-1 belongs to a highly conserved gene family, composed of three exons and

alternatively translated into the endoplasmatic reticulum (ER) as a full-length 178 amino acids alpha-isoform and a beta-isoform truncated by the first 32 amino acids at the N-terminus which is derived from an alternative translation start[72] (Fig. 7A) and is co-expressed with caveolin-2 in cells and tissues of mesenchymal, endo/epithelial, neuronal/ glial origin.[73] Cav-1 is believed to have a membrane spanning unique hairpin conformation where both C- and N-termini are exposed to the cytosol (Fig. 7B).

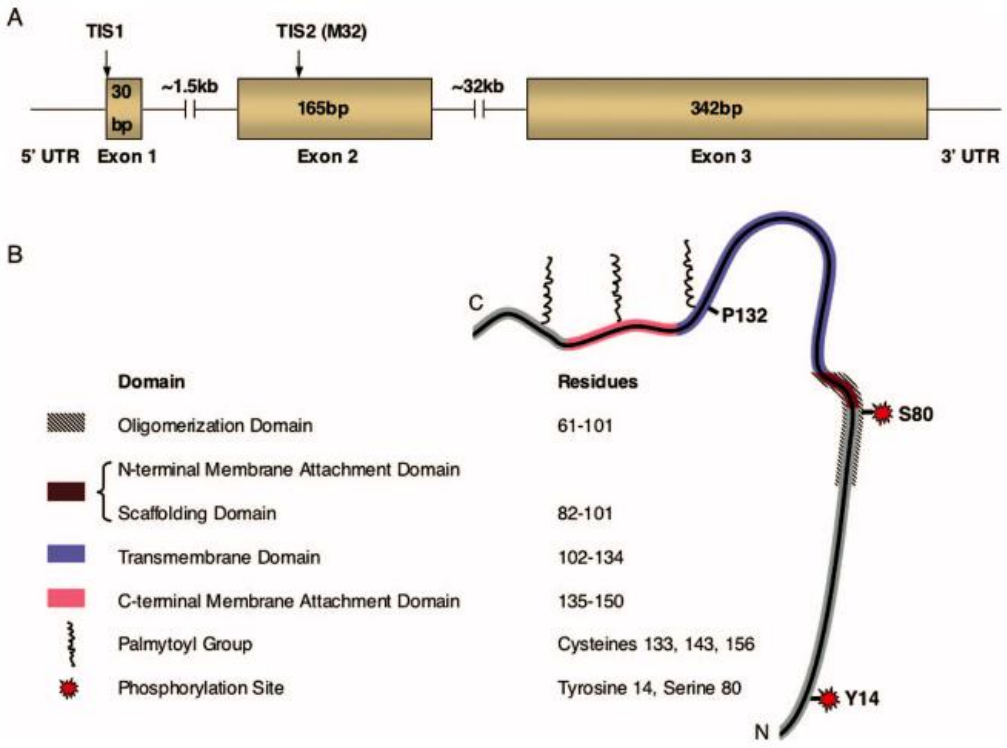

Fig. 7 Schematic structure of Cav-1 gene and protein.[74]

Cav-1, via its scaffolding domain (CSD) (amino acids 82–101) interacts with a variety of specific partner proteins binds short peptide motifs that rich in aromatic residues such as $\omega x_4 \omega x_2 \omega$ (ω = aromatic acid, x = any amino acid).[75] Other important domains include an oligomerization domain (amino acids 61–101) of Cav-1 monomers assemble into high-molecular weight homo- and hetero-oligomers (with caveolin-2) to form the striated caveolar coat structure (Fig. 8).

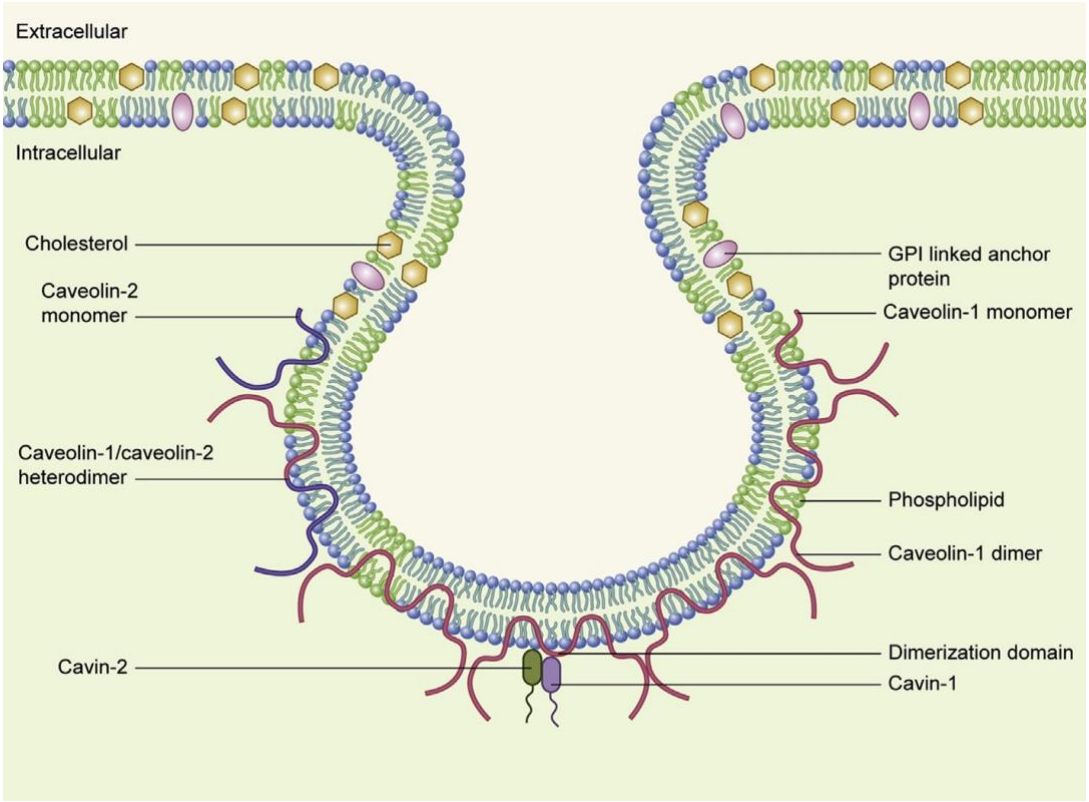

Fig. 8 Caveolin oligomer formation is regulated due to interaction with cavin members. Cav-1 and cav-2 can exist as monomers, homodimers, or heterodimers. The presence of both Cavin-1 and Cavin-2 allows Cav-1 or Cav-2 to interact within the cell membrane to form hetero-oligomers in caveolae. In the absence of Cavin-1 or Cavin-2, caveolin oligomers embedded in the cell membrane cannot contribute to caveolae formation. (taken from [76])

1.8 Role of Cav-1 in cancer progression and in GBM

Over the past 10-15 years, Cav-1 has been found to have oncogenic and metastasis promoting roles, however, others have described opposing roles of being either a tumour suppressor or an oncogene depending on the tumour type or tissue of interest.[77-79] Down-regulation of Cav-1 expression is observed previously in breast, colon, lung and ovarian cancer. Thus, oncogenic transformation of cells was associated with reduction of Cav-1 expression, and antisense-mediated down-regulation of Cav-1 expression was sufficient to drive oncogenic transformation in NIH 3T3 cells. Moreover, exogenous expression of Cav-1 in oncogenically transformed cells and cancer cell lines inhibited cell growth and tumorigenesis. This evidence indicates that Cav-1 can act as a tumour suppressor. In contrast, other studies have reported that Cav-1 expression was up-regulated in human cancers in association with metastases and poor prognosis. These results suggest that Cav-1 can function as an tumour promoter as well.[80] The tumour-promoting role of Cav-1 in metastasis is assumed to be based on its

general role in enabling and supporting membrane viscosity/fluidity and cell motility.[81] Cav-1 has been validated as a participating protein that is targeted to zonula adherens (Adherens junction, ZA) and zonula occludens (Tight junction, TJ), to stabilize them in order to maintain epithelial[82, 83] and endothelial barriers *in vitro*[84] and *in vivo* (e.g. blood–brain-barrier[13]). Metastasis involves a loosening of both cell–cell and cell–matrix contacts and degradation of the extracellular matrix (ECM) to promote cell motility and invasion. In addition Cav-1 seems to play a role in the angiogenic process, as confirmed by knock-down of Cav-1 expression by antisense oligonucleotides[85] or RNAi-based approaches[86], resulting in blockage of angiogenesis.

Interestingly, one of the most frequent point mutants in GBM occurs in the tumour suppressor protein, p53.[87] in certain p53- mutant tumours, glucose restriction, which induces oxidative stress, resulted in activation of autophagy and an autophagy-dependent degradation of mutant p53, leading to a feed forward acceleration of autophagy and tumour inhibition.[88] Furthermore, in the tumour stroma, Cav-1 expression has been found to be similarly downregulated by oxidative stress when autophagy was activated, which, in turn, resulted in a feedforward upregulation of stromal autophagy.[89] Termed the "reverse Warburg effect," this tumour microenvironment is defined by enhanced stromal aerobic glycolysis, oxidative stress and localized inflammation, which, in turn, promotes tumour cell survival through cancer cell parasitism of nutrients released from the autophagic stromal cells. Collectively, these results suggest that the expression levels of Cav-1, and certain mutant forms of p53, may be regulated in a similar fashion by autophagy, leading, however, to different phenotypic outcomes depending upon whether their expression occurs in the tumour or in the stromal component.[88-90]

The most commonly silenced genes TP53 and the tumour suppressor proteins PTEN in GBM involve antagonizing the PI3K/AKT/mTOR pathway and regulate cell cycle, which react to DNA damage and cell death, respectively. Notably, these two genes are highly upregulated in cells overexpressing Cav-1. This explains the gene signatures connected to downregulation of signalling pathways as well as reduced invasiveness.[91]

Cellular senescence is a powerful tumor suppressor mechanism. In the literature, it was shown that Cav-1 promoted stress-induced premature senescence in fibroblasts through the

modulation of Mdm2, ATM, PP2A-C, Nrf2, and Sirt1 functions. Thus, it remains unexplored whether Cav-1 regulates the tumor suppressor properties of oncogene-induced senescence. Around two decades ago, it was shown that overexpression of oncogenic H-Ras (H-RasG12V) in normal cells was enough to induce cellular senescence instead of increasing cell proliferation. Studies have demonstrated that senescence happens in premalignant lesions in several mouse cancer models, including lymphoma, prostate, mammary and lung carcinoma. Additionally, senescence was found in benign lesions of the prostate, skin and neurofibromas in human and was associated with oncogenic mutation of BRAF, PTEN inactivation and NF1 mutations. In this way, cellular senescence is activated by the same oncogene that leads the initial tumorigenesis to progress the cancer.[92]

Genetic evidence emerging from gene mapping studies revealed that the human Cav-1 gene maps to the long arm of human chromosome 7 (7q31.1). This region, the D7S522 locus, encompasses a known fragile site (FRA7G) and is often associated with loss of heterozygosity (LOH) in various cancers. The deletion of this region and its association with the pathogenesis of several different types of cancers lends credible support to the presence of a tumor suppressor gene within this genetic locus. While no genes have been directly mapped to the D7S522 locus, the closest genes to this region encode caveolin-2 and Cav-1.[93-95]

Overexpression of Cav-1 in cultured cells is sufficient to inhibit signalling from several proliferative pathways. For instance, it has been shown that key components of the Ras-p42/44 MAP kinase cascade (MEK and ERK) reside within caveolae and other members of this signaling cascade are negatively regulated by a direct interaction with Cav-1. It has also been demonstrated that transient transfection of Cav-1 dramatically inhibits signalling along the Raf-1/MEK/ERK pathway, and the kinase activity of MEK-1 and ERK-2 are inhibited by incubation with Cav-1 scaffolding domain-based peptides in vitro[23, 96]

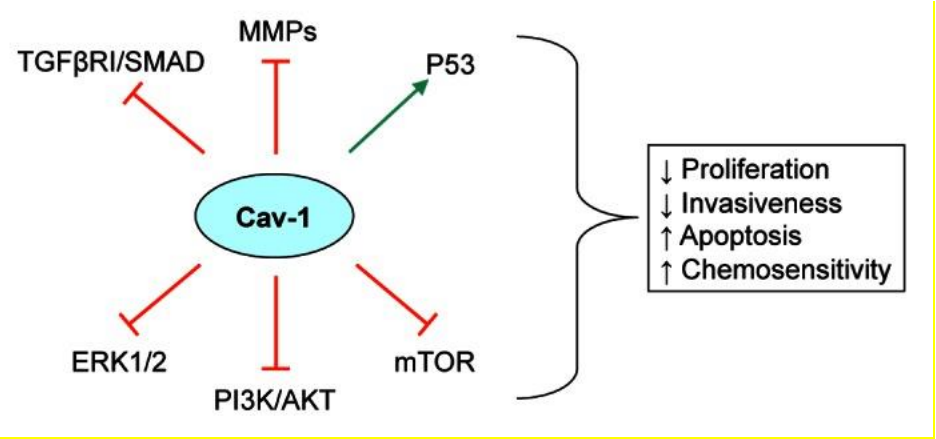

Fig. 9 Schematic diagram of various role of Cav-1. Red lines denote genes or pathways inhibited by Cav-1, while green lines indicate those that are upregulated.[97]

In recent publication, Talasia et al. performed the human gene v1.0 ST microarray on xenograft tissues. They harvested tumors until those reached similar sizes by observing with MRI. At the same time, tissues containing >90% tumors were harvested for RNA isolation. Microarray analysis revealed six hundred forty-five genes differentially expressed between the phenotypes. Among them top 30 genes mostly deregulated between the two groups were also isolated (Fig. 10).[98] The analysis of associations of gene expression with biological functions, revealed that the genes upregulated in the angiogenic xenografts indeed are involved in angiogenesis, response to wounding, and response to cellular stress. In the gene expression data, they also showed that Cav-1 is one of the top genes among other genes that upregulated in the mesenchymal subtypes. Thus, it is still unclear whether Cav-1 is a tumor suppressor or promotor in GBM.

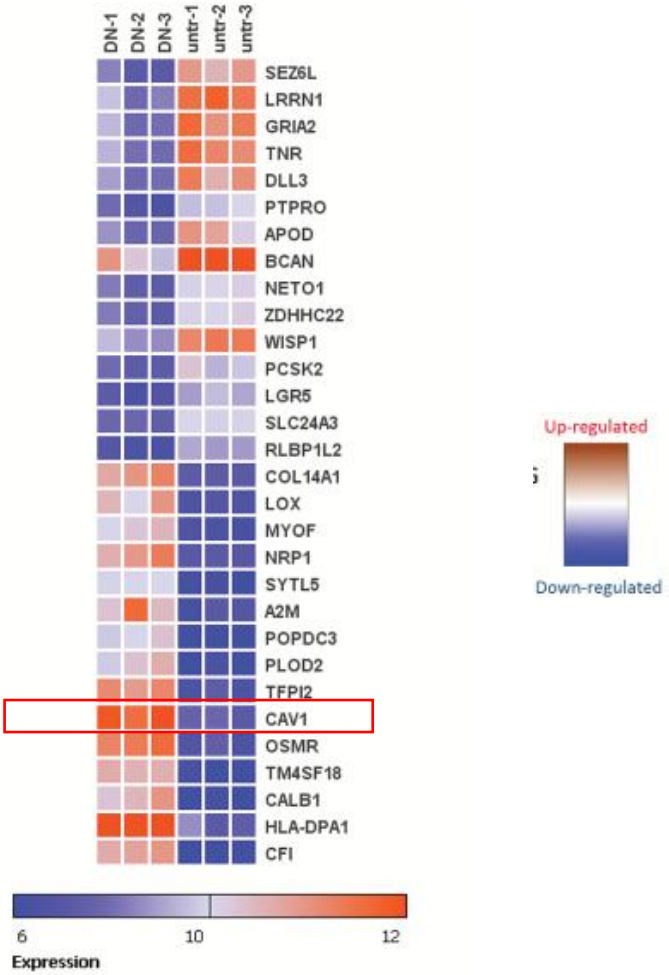

Fig. 10 The gene expression data show that the angiogenic switch is linked to proneural-to-mesenchymal transition in GBM (taken from[98]). Shown are the highest differentially expressed genes between invasive EGFR amplified cells and tumors transduced with EGFR-DN resulting in angiogenic tumours of the mesenchymal subtype. Among 30 genes, Cav-1 is one of the top genes that is upregulated in the mesenchymal subtype.

2. Aims

We aim to develop this project by adopting the following strategy:

1. Analyse TCGA data for correlation/anticorrelation of mesenchymal/proneural markers with Cav-1

2. Analyse expression patterns of Cav-1 in GBM patient samples

3. Analyse HIF-1α expression under normoxia and hypoxia in patient-derived primary GBM cell lines

4. Test the efficacy of digoxin to block HIF-1α upregulation under hypoxia

5. Evaluate Cav-1 expression under normoxic and hypoxic conditions in patient-derived primary GBM cell lines by western blotting

6. Analyse expression of proneural and mesenchymal markers under normoxia and hypoxia by western blotting.

3. Materials and Methods

The project was conducted from August 2017 to May 2018 at the Department of Biomedicine, University of Bergen, Norway.

3.1 List of materials

Table 2: Experimental cell lines

Cell line	Type	Supplier
BG5	GBM	Haukeland Hospital, Bergen, Norway
BG7	GBM	Haukeland Hospital, Bergen, Norway
GG14	GBM	University Medical Center Groningen, Netherlands
GG16	GBM	University Medical Center Groningen, Netherlands
S24	GBM	German Cancer Research Center (DKFZ), Heidelberg

Each experimental cell lines were cultured in two micro-environmental conditions - normoxia and hypoxia.

Table 3: General chemicals and solutions

Chemical/solutions	Catalogue no.	Supplier
Methanol (100%)	1060092500	Sigma-Aldrich, St. Louis, Missouri, USA

Ponceau	P3504	Sigma-Aldrich, St. Louis, Missouri, USA
Soduim cloride (NaCl)	S0390	Sigma-Aldrich, St. Louis, Missouri, USA
Ethanol, absolute	32221	Sigma-Aldrich, St. Louis, Missouri, USA
Dulbecco's Phosphate Buffered Saline (10x) (PBS)	D1408	Sigma-Aldrich, St. Louis, Missouri, USA
Accutase	A6964	Sigma-Aldrich, St. Louis, Missouri, USA
Neurobasal medium(NBM)	21103-049	Gibco, Thermo Fisher Scientific, Waltham, MA, USA
bFGF (Fibroblast Growth Factor-basic)	100-18B	Peprotech, Germany
B27	17504-044	Thermo Fisher Scientific, Waltham, MA, USA
EGF (Epidermal Growth Factor)	236-EG-200	R & D System
Virkon tablets for decontamination	VIRKTABS	Wilmington, Delaware, USA

Table 4: Reagents for western blotting

Reagents	**Catalogue number**	**Supplier**

M-PER Mammalian Protein Extraction Reagent kit	78503	Thermo Fisher Scientific, Waltham, MA, USA
Protease and Phosphatase Inhibitor Cocktail(100X)	78440	Thermo Fisher Scientific, Waltham, MA, USA
NuPAGE® ™ Antioxidant	NP0005	Invitrogen by Thermo Fisher Scientific
NuPAGE® ™ 4-12% Bis-Tris Gel (15 wells)	NP0323	Invitrogen by Thermo Fisher Scientific
NuPAGE® ® (4-12% gradient Bis-Tris gels (10wells)	NP0321	Invitrogen by Thermo Fisher Scientific
NuPAGE® Sample Reducing agent (10X)	NP0004	Invitrogen, Carlsbad, California, USA
SeeBlue® Plus2 Prestained Standard (1X)	LC5925	Invitrogen, Carlsbad, California, USA
NuPAGE® LDS sample buffer (4X)	NP0007	Invitrogen, Carlsbad, California, USA
NuPAGE® MOPS SDS Running buffer (20X)	NP0001	Novex by Life Technoogies
NuPAGE® Transfer buffer (20X)	NP0006-1	Novex by Life Technoogies
Super Signal® West Femto	34096	TFS
Super Signal® West Pico	34080	TFS
Triton ™ X-100	9002-93-1	Sigma-Aldrich, St. Louis, Missouri, USA

Tween 20	9005-64-5	Sigma-Aldrich, St. Louis, Missouri, USA
Tris Base	648310	Merck Chemicals, Darmstadt, Germany
Nitrocellulose transfer membrane (0.2 μm)	10600001	GE Healthcare, Pittsburgh, PA, USA
DifcoTM Skim milk powder	232100	BD Biosciences, Franklin Lakes, NJ, USA
Bovine serum albumin (BSA)	A4503	Sigma-Aldrich, St. Louis, Missouri, USA

Table 5: Reagents for immunostaining

Reagents	**Catalogue no.**	**Supplier**
Prolong Gold antifade reagent with DAPI	P36935	Molecular probes, USA
Corning® Matrigel® Matrix Growth Factor Reduced (GFR) Basement Membrane Matrix	356230	Corning Incorporated Life Sciences, Tewksbury, MA 01876
Normal goat serum (1:50)	-	Dako Denmark A/S, Glostrup, Denmark

Table 6: Primary antibody for immunostaining

Name	Catalogue no.	Dilution	Dilution buffer	supplier
HIF1A	51608	1:500	PBS + BSA	Abcam

Table 7: Secondary antibody for immunostaining

Name	Catalogue no.	Dilution	Dilution buffer	supplier
Goat anti-mouse Alexa 488 (green)	A10235	1:200	PBS + BSA	Thermo Fisher Scientific, Waltham, MA, USA

Table 8: Inhibitor for immunostaining

Name	CAS No.	Supplier
Digoxin	20830-75-5	Axon Medchem

Table 9: Primary antibody for WB

Source of the primary antibody is rabbit for all except, Anti EZH2 and Anti HI1-A (both of them are from mouse) and Anti-YKL40 (from goat).

Name	Catalogue No.	Dilution	Molecular Weight (KDa)	Blocking buffer	Supplier

Anti-PDGFRA	31645	1:1000	195	Milk	Cell signalling Technology, USA
Anti-PSTAT3	9134p	1:1000	86	BSA	Cell signalling Technology, USA
Anti-EZH2	3147	1:1000	98	Milk	Cell signalling Technology, USA
Anti-YKL40	30465	1:500	40	Milk	Santa Cruz Biotechnology
Anti-HIF1A	51608	1:1000	120	Milk	Abcam
Anti-Cav1	2910	1:1000	21,24	Milk	Abcam
Anti-Olig2	9610	1:5000	32	Milk	EMD Millipore
Anti-BMI	05-637	1:1000	37	BSA	EMD Millipore
Anti-CD44	7923	1:2000	82	Milk	Sigma Aldrich
Anti-HIF1A	610959	1:250	120	Milk	BD Translab
Anti-GAPDH	9485	1:5000	37	BSA	Abcam

Table 10: Secondary Antibodies for WB

All the secondary antibodies were supplied by Thermo Fisher scientific, Waltham, MA, USA except anti-goat IgG-B, which is from Santa Cruz Biotechnology, INC

Name	Catalogue No.	Animal of origin	Dilution	Blocking buffer
Anti-rabbit HRP	31462	Goat	1:10,000	BSA/Milk
Anti-goat IgG-B	2042	Donkey	1:5000	BSA
Anti-mouse HRP	31430	Mouse		BSA/Milk

Table 11: Equipment for all experiment

Equipment	Supplier
Power Pac 300 electrophoresis power supply	164-5050 Bio-Rad, Hercules, CA, USA
Nikon E100 Light microscope	Nikon Instruments, Tokyo, Japan
Fluorescence microscope	3512000236, Zeiss AXIOZ1, Germany
Holten laminar airflow clean benches	SANYO Electric Co, Osaka, Japan)
Luminescent Image Analyzer LAS (3000) Fujifilm UV intelligent dark box	4622724, Fujifilm Medical Systems Inc., Stamford, CT, USA
Cell culture CO2 incubator	Panasonic Healthcare Co. Ltd. Sakata, Japan
Hypoxia C-chamber	Panasonic Healthcare Co. Ltd. Sakata, Japan
Inverted Microscope	TS100/TS100F, Biocompare, USA
Eppendorf centrifuge 5424 R	Eppendorf, Hamburg, Germany
Versa Max Microplate Reader	Molecular devices, Sunnyvale, CA, USA
Direct Detector™ Spectrometer	DDHW00010-WW, Merck Millipore, USA

Trans-Blot Turbo™ Transfer System	Bio-Rad, Hercules, CA, USA
SH800Z Cell Sorter	Sony Biotechnology, Japan
Automated cell counter NucleoCounter® NC-200™	ChemoMetec A/S, Denmark
SimpliAmp Thermal Cycler	Thermo Fisher Scientific, Waltham, MA USA
Cellular RNA detection, Bioanalyzer System	2100, Agilent Technologies, Waldbronn, Germany
Heraeus Multifuge 3SR Plus Centrifuge	DJB Labcare, Thermo Fisher Scientific, UK

3.2 Recipes for used buffers

Neurobasal Medium (NBM): NBM is supplemented with B27, L-Glutamax, penicillin-streptomycin, heparin, 20ng/ml bFGF (Fibroblast Growth Factor-basic) and 20ng/ml EGF (Epidermal Growth Factor),

Phosphate buffered Saline (PBS): Dulbecco's Phosphate Buffered saline (PBS, 10x) is diluted at a concentration of 10% v/v volume of in 9 volumes of autoclaved Milli-Q water.

Cell-freezing medium: 10% v/v DMSO and 20% v/v heat inactivated foetal bovine serum (FBS) were added to DMEM.

4 % v/v Para formaldehyde (PFA) solution: Fixation reagent was prepared by adding 1 volume of 16%v/v PFA solution in 3 volumes of 1x PBS.

Ponceau S: 0.1% w/v Ponceau stain was added in 5 % v/v acetic acid

SDS-PAGE running buffer: 50 ml of 20X MOPS was diluted with 950 ml of Milli-Q water and 500 µl NuPAGE® antioxidant.

Transfer buffer: 50ml of 20% NuPAGE® transfer buffer, 100ml of methanol, 1ml of NuPAGE® antioxidant were mixed to 849ml of milli-Q water.

Western blot wash buffers: For 1 litre (TBS) 10x: 20 Mm Tris-HCL, 0.15 M NaCl is mixed in 900ml of Milli- Q followed by adjustment of pH at 7.6.

TBST (1%): 100 ml TBS(10X) is mixed with 900ml milli-Q water and 1ml Tween.

Western blot blocking buffer: 5% w/v skim milk powder TBST and 5% w/v BSA TBST.

3.3 Methods

3.3.1 Cell culture

Fresh Human Glioblastoma samples were processed for cell cultures within 1 hour after reception. As reference material for all experiments, the glioblastoma cells (GBM) were routinely cultured as neurosphere in 75 cm^2 culture flasks (Nunc, Thermo Fischer Scientific, Waltham, Massachusetts, USA) in Neurobasal medium, supplemented with necessary ingredients as described in section 3.2**.** Glioblastoma cell lines were kept at 37 ^{0}C in tissue culture incubators at 100 % humidity with 5 % CO_2 and 95 % air. For hypoxia treatment, cells were first maintained in the regular normoxic incubator for around 12 hours. The idea of giving some time following disccociation of the spheroids is to let them overcome the stress caused by accutase and mechanical dissociations by repeated pipetting. Therafter the flasks were transferred to the Hypoxia C-chamber, (Panasonic Healthcare Co. Ltd. Sakata, Japan) filled with 1% O_2, 5% CO_2 and 94% N_2, at 98% humidity and 37 °C.

3.3.2 Passaging

The cells were cultured generally at 70-90% confluency and passaged almost once a week to avoid overgrowth. Old medium was removed by centrifugation at 400 rpm for 5 minutes and cells were washed twice with 1x phosphate buffered saline (PBS). Neurospheres were dissociated by incubation at 37 ^{O}C in Accutase (Cat. No A6964, Sigma Aldrich) for around 3-5 minutes. Accutase was inactivated by adding supplemented Neurobasal Medium (NBM), (Gibco, Cat. No. 211103-049). Supernatant were discarded and 15 ml of fresh NB medium was added. The cell suspension was gently pipetted up and down to dissociate the spheroids and

produce a solution of single and rounded cells under the microscope. Passage number, owner's name and date were registered each time the cells were passaged. Passaging of cells was carried out in a laminar flow bench (SANYO Electric Co, Osaka, Japan) that was sterilized with 70 % ethanol before and after use. Cells were visualized using an inverted light microscope.

3.3.3 Cryopreservation of cells

Cells were frozen down for cryopreservation after 4 passages. Cells were gently detached and a single cell suspension was made. Then, the cell suspension was transferred to a 15ml centrifuge tube and centrifuged at 900rpm for 5 minutes. After discarding the supernatant, pelleted cells were re-suspended in RT (10% v/v DMSO, 10% v/v foetal bovine serum complete medium). The cells were homogenously mixed and transferred to cryovials. Cryo-vials were marked with name of the cell line, passage number, date, and name of owner and placed in an isopropanol containing box at room temperature. Cells in isopropanol box were stored at –80°C for overnight. Frozen cells were then transferred to the liquid nitrogen tank for long-term storage.

3.3.4 Thawing of cells

Cells were collected from the N_2 tank, and transported in ice box and thawed by placing the cryotubes in a 37 ^{O}C water bath gently. Immediately after thawing, the cell suspension was transferred to a 15ml tube and washed with 5ml of PBS and centrifuged at 900 rpm for 5 minutes. After discarding the supernatant, pelleted cells were re-suspended in 6-7 ml of NBM. After 24 hours incubation at 37 ^{O}C, the medium was changed to remove remnants of freezing solution which may otherwise harm the cells.

3.3.5 Cell counting

Cells were rinsed with 5 ml of 1x PBS and treated with 1ml of accutase. The flask was incubated for 3-5 minutes in the incubator (37 ^{O}C and 5% CO_2) according to the size of the cell pellet. Approximately 10 ml of NBM was added in the culture flask, pipetted up and down gently and then the suspension was filled into a falcon tube. 100 µl cell suspension was

transferred into an eppendorf tube for cell counting by Automated cell counter NucleoCounter® NC-200™.

3.3.6 SDS-PAGE and western blotting

Western blotting is a widely used technique for identification of specific proteins from the complex mixture of proteins extracted from cells. Protein is separated by SDS-PAGE (sodium dodecyl sulfate polyacrylamide gel electrophoresis) based on their molecular weight, size and ability to bind to specific antibodies.

Later, Proteins are transferred to a nitrocellulose membrane producing a band for each protein followed by incubation with epitope specific primary and secondary antibodies that binds to the particular proteins on the membrane. The unbound antibody is washed off leaving only the bound antibody to the protein of interest. Finally, the bound antibodies are then detected by the image, which is processed by chemiluminescent agent and visualized by a luminescent image analyser.

Immunoblotting is a semi quantitative technique that provides a relative comparison of protein levels rather than absolute measure of quantity. Housekeeping protein GAPDH are used as loading control.

3.3.7 Isolation of protein

Old media was removed which was transferred to the 15ml tube and cells were washed twice with 10-12 ml of ice-cold 1x phosphate buffered saline (1xPBS) followed by centrifuged at 3000 rpm for 3-4 minutes in 2 ^{0}C. According to the method, 150-200µl protein lysis buffer (M-PER with Protease and phosphatase inhibitor single use cocktail) was added in the cell pellet (depending on size of the cell pellet). The cell-lysis buffer suspension was transferred to a 1.5 ml eppendorf tube and incubated for 30 minutes. The whole protein collection procedure was maintained on ice for both conditions, normoxia and hypoxia, to avoid protein degradation. Subsequently, the samples were then centrifuged for 15 minutes at 4 ^{o}C and maximum speed (14,000 rpm) in an eppendorf micro centrifuge. This accumulates the cellular debris into a pellet at the bottom of the eppendorf tube. Then, the supernatant, which contains the protein was collected and transferred to a new eppendorf tube and stored at -80°C until use.

3.3.8 Determination of protein concentration

The concentration of protein sample concentration was acquired using IR-based Direct Detect® assay-free sample cards (Catalogue No. DDAC00010-8P) (version 2.0). All measurements were performed using 2µL of sample solution per membrane position. Normal lysis buffer was used as a standard and the test sample was loaded in triplicates. Unknown protein mixtures were analysed in the "Relative Absorbance" mode, where the system delivers information based solely on IR signal strength by Direct Detect® spectrometer (Catalogue No. DDHW00010-WW). Empirical sample concentration values were determined by interpolation from calibration curves developed for each specific protein.

3.3.9 Sample preparation and SDS-PAGE

Samples were prepared for SDS-PAGE, where 20-25µg of protein samples was mixed with 7.5µl of 4x LDS sample buffer and 1µl of reducing agent and distilled water was added until the total volume reached 20µl. The mixture was heated for 10 minutes at 75 ^{O}C. After sample preparation, the extract is ready to be loaded to separate the proteins according to size by gel electrophoresis. Precast NuPAGE® (1.5 mm) 4-12% gradient Bis-Tris gels were used to separate the polypeptides by size. SDS denatures the protein's tertiary structure and transforms to a linear shape and provides a negative charge that make them migrate towards the positive pole in electrophoresis. The white tape at the bottom of the gel cassette was removed and then placed in the slot of the Novex® mini-cell gel chamber (Invitrogen). The chamber of the tank was blocked by a barrage and locked. The inner chamber was assembled first and filled with freshly prepared 50ml 1X NuPAGE® MOPS Running Buffer including 500µl of antioxidant and the outer chamber was filled with of previously used running buffer (approximately 450 ml). The comb of the wells was removed carefully by pulling upward. Subsequently, 10µl of SeeBlue® plus2 pre-stained protein standard ladder followed by 10µl of sample mixture was loaded in each well. The lid was fit onto the tank and plugged into the power source and the electrophoresis was run for about one and half hour (150V). Electrophoresed gel was drawn from the gel cassette and the tank was rinsed with UF (Ultrafiltration) water.

Table 12: Loading mixture for SDS-PAGE

Reagent	Reduced sample
Sample	x µl
Tris-Glycine SDS Sample Buffer (2X)	5 µl
NuPAGE® Reducing agent (10X)	1 µl
Deionized water	to 4 µl
Total volume	10 µl

3.3.10 Procedure of electron transfer of proteins

In electrophoretic transfer, an electric field was employed to elute the proteins from electrophoresed gel and transfer them to the nitrocellulose membrane (blotting). A set of blotting sponge pads, filter paper, the SDS-Gel, 0.2 µm nitrocellulose membrane were soaked in transfer buffer and assembled in the way as shown in (Fig.1). Air bubbles formed between the gel and the nitrocellulose membrane were removed by gentle rolling using the roller tool. The transfer chamber was transferred to a Xcell Sure Lock mini-cell chamber (Invitrogen). The transfer chamber was filled with freshly prepared transfer buffer and the outer chamber was filled with pre-used transfer buffer. The lid was fit onto the mini gel chamber. Finally, the Xcell Sure Lock mini-cell gel chamber was placed on the ice and electrophoresis was run at 37 V for 90 minutes. After completing the run, the nitrocellulose membrane was collected carefully.

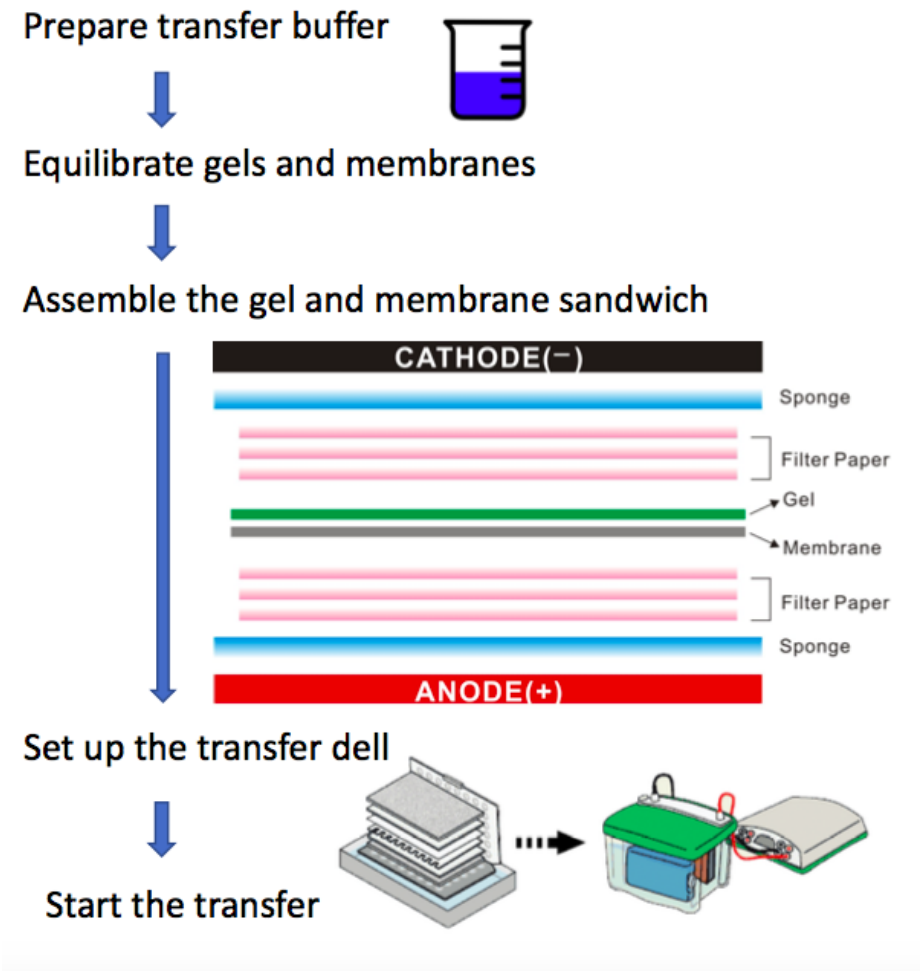

Fig. 11 Schematic diagram of electron transfer procedure of protein.

3.3.11 Ponceau S staining

After blotting, the nitrocellulose membrane was washed in MilliQ-H_2O followed by incubation in 0.1% w/v Ponceau S dye for 5 minutes at room temperature to verify that the protein had been transferred to the membrane properly. Ponceau S is a coloured dye that binds reversibly to proteins and allows to check the efficiency of transferring. Thereafter, the membrane was rinsed with MilliQ-H_2O and the membrane was cut according to molecular weight of the target protein.

3.3.12 Blocking, antibody incubation and detection

The nitrocellulose membrane was washed in desired amount of washing buffer 1x TBS in room temperature. Then the membrane was cut according to the desired bands and incubated with blocking buffer for 1 hour on a shaker in room temperature to avoid

nonspecific binding (5% skim milk or BSA (for phosphoprotein) in 1x TBST). The blots were incubated with specific primary and secondary antibodies respectively to visualize the desired proteins. The antibodies were also diluted (as mentioned in the Table 9) in blocking buffer. Thereafter, the blots were incubated with primary antibody solution with agitation overnight at 4 ^{o}C. On the following day, blots were rinsed 4 times in 1x TBST before adding secondary antibodies, 5 minutes each at room temperature. After that, the blots were incubated with the HRP labelled secondary antibody (Table 10) for 1 hour. gentle shaking at RT and washed again 4 times for 5 minutes with 1x TBST before chemiluminescent detection.

3.3.13 Chemiluminescence and quantification of protein expression

Blots were developed with the SuperSignal® West Femto as well as SuperSignal® West Pico (Maximum Sensitivity Substrate Chemiluminescent Substrates). The kit contains an enhanced chemiluminescent substrate for antibody conjugated horseradish peroxidase (HRP) enzyme used for immunoblotting. The blots were allowed to absorb the substrate for five minutes before drained the excess wash buffer from the membranes. The development was done with a luminescent image analyser, Image Reader LAS-3000 (Fujifilm Medical Systems Inc., Stamford, Connecticut, USA). Subsequently, the relative expression levels of the proteins were quantified using ImageJ software. Finally, the relative density was calculated and analysed for all the samples. The housekeeping gene GAPDH (Glyceraldehyde-3 phosphate-dehydrogenase) was used as a loading control to confirm equal amount of protein was loaded.

3.3.14 Immunocytochemistry

Immunocytochemistry (ICC) is a technique for detecting a protein of interest inside or on the membrane of cells. The protein is identified by using an antibody conjugated to a fluorescent tag – a fluorophore. Immunostaining can then be investigated using different techniques, for example fluorescence microscopy and confocal microscopy. One can distinguish between direct and indirect ICC. In direct ICC, only a primary fluorophore-conjugated antibody is used. In indirect ICC, a primary antibody is allowed to bind to the target protein first, and then a secondary fluorophore-conjugated antibody binds to the primary antibody. Indirect

ICC is more sensitive because several secondary antibodies can bind to a single primary antibody, thus enhancing the signal.

3.3.15 Preparation of cells for immunostaining and Matrigel coating

Cell culture was done in 1% O_2 and 21% CO_2 (Hypoxia) and in the standard tissue culture incubator. Cells were kept on ice after removal from the hypoxia chamber. Following the normal procedure of cell culture the cells were splitted for fixation. Prepared desired amount of Matrigel matrix (Corning Matrigel matrix is a reconstituted basement membrane preparation that is extracted from the Engelbreth-Holm-Swarm (EHS) mouse sarcoma, a tumor rich in extracellular matrix proteins) which was diluted in NB medium (Neurobasal medium) without growth factors. Subsequently, Matrigel coating was done by pipetting 2 ml droplets of the mixture (NB medium + matrigel) solution onto 18 x 18 mm glass cover slips in 6-well plates (which was planned for normoxia, hypoxia and hypoxia with inhibitor in different concentrations) and incubated for 30 minutes at 37 ^{o}C.

3.3.16 Procedure of Immunostaining

Cells cultured on poly-L-lysine (Sigma-Aldrich)-coated coverslips were fixed for 10 min using 4% formaldehyde or 100% methanol. After 3 times washing with cold PBS, cells were permeabilized with 0.1% Triton (Sigma-Aldrich) in PBS, washed again with PBS followed by a blocking step for 1 hour with PBS + 0.1% Tween-20 (Sigma-Aldrich), 2% bovine serum albumin (BSA) and 1: 50 dilution of normal goat serum (Dako Denmark A/S, Glostrup, Denmark). Subsequently, cells were incubated with the indicated primary antibody HIF1A (diluted 1:500 in dilution buffer) at room temperature for 1.5 hours. After 3 times washing with PBS, slides were incubated for 1 h with the appropriate secondary antibody, goat anti-rabbit Alexa 488 (light sensitive) (diluted 1:200 in dilution buffer). After washing 3x5 times with PBST and 2x5 times with PBS, the cover slips were mounted on microscope slides 25x75x1 mm with 5μM of Prolong Gold antifade reagent containing DAPI (DAPI stains the nucleus of the cell by binding to DNA). The mounting solution was allowed to dry for overnight at RT in dark. Cells were examined by fluorescent microscopy (Leica DM6000, Leica Microsystems GmbH, Mannheim, Germany) and images were captured using Leica DFC360 FX camera.

3.3.17 Immunohistochemistry

Formalin fixed paraffin-embedded 3 μm thick consecutive tissue sections were mounted on microscope slides and dried overnight at 55 °C. Tissue sections were deparaffinized in xylol and rehydrated in graded series of ethanol, and stained with hematoxylin and eosin (HE). Tissue labelling was performed using the DiscoveryXT immunohistochemistry system (Ventana/Roche, Strasbourg, France). Antigen retrieval was performed using microwave pre-treatment in pH 6.0 citrate buffer. Sections were treated with 0.3% H_2O_2 for 30 min and blocked for 1 h with 2% BSA to reduce non-specific primary antibody binding. Next, incubated with the primary antibody anti-caveoline-1 (rabbit) overnight at 4 °C.

As negative controls, primary antibodies were omitted. After incubation with primary antibody, secondary rabbit anti-goat IgG (H+L) antibody were used. Staining was visualized by 3,3′-diaminobenzidine and sections were counterstained with hematoxylin and mounted. Images of relevant sections were acquired using a C9600 NanoZoomer (Hamamatsu Photonics KK, Hamamatsu City, Japan).

4. Result

4.1 Cav-1 expression and correlation with mesenchymal and proneural markers in GBM TCGA data.

The analysis of GBM TCGA data using the online tool "betastasis.com" showed a correlation of Cav-1 expression with mesenchymal markers CEBPB, CD44, CHI3L1 (YKL40) and STAT3 (Fig. 12). In contrast, analysis of proneural markers olig2, DLL3, ASCL1 and PDGFRA showed anti-correlation with Cav-1 expression (Fig. 13). This indicated that Cav-1 might be upregulated in GBM of the mesenchymal subtype.

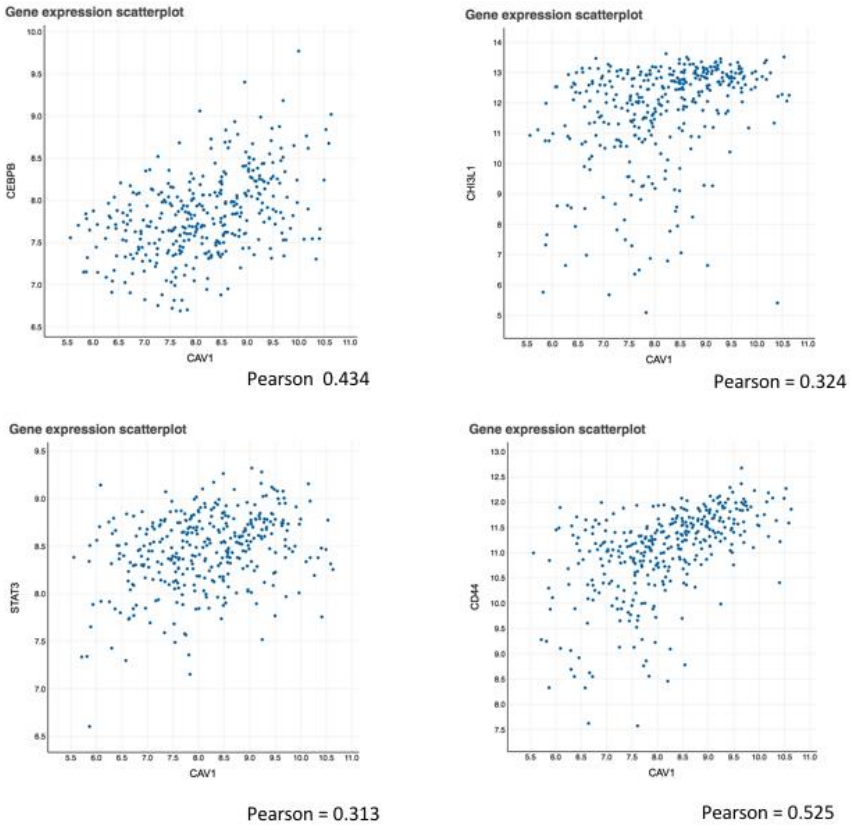

Fig. 12 GBM TCGA analysis of mesenchymal markers and correlation with Cav1 expression. Pearson correlation co-efficient is indicated.

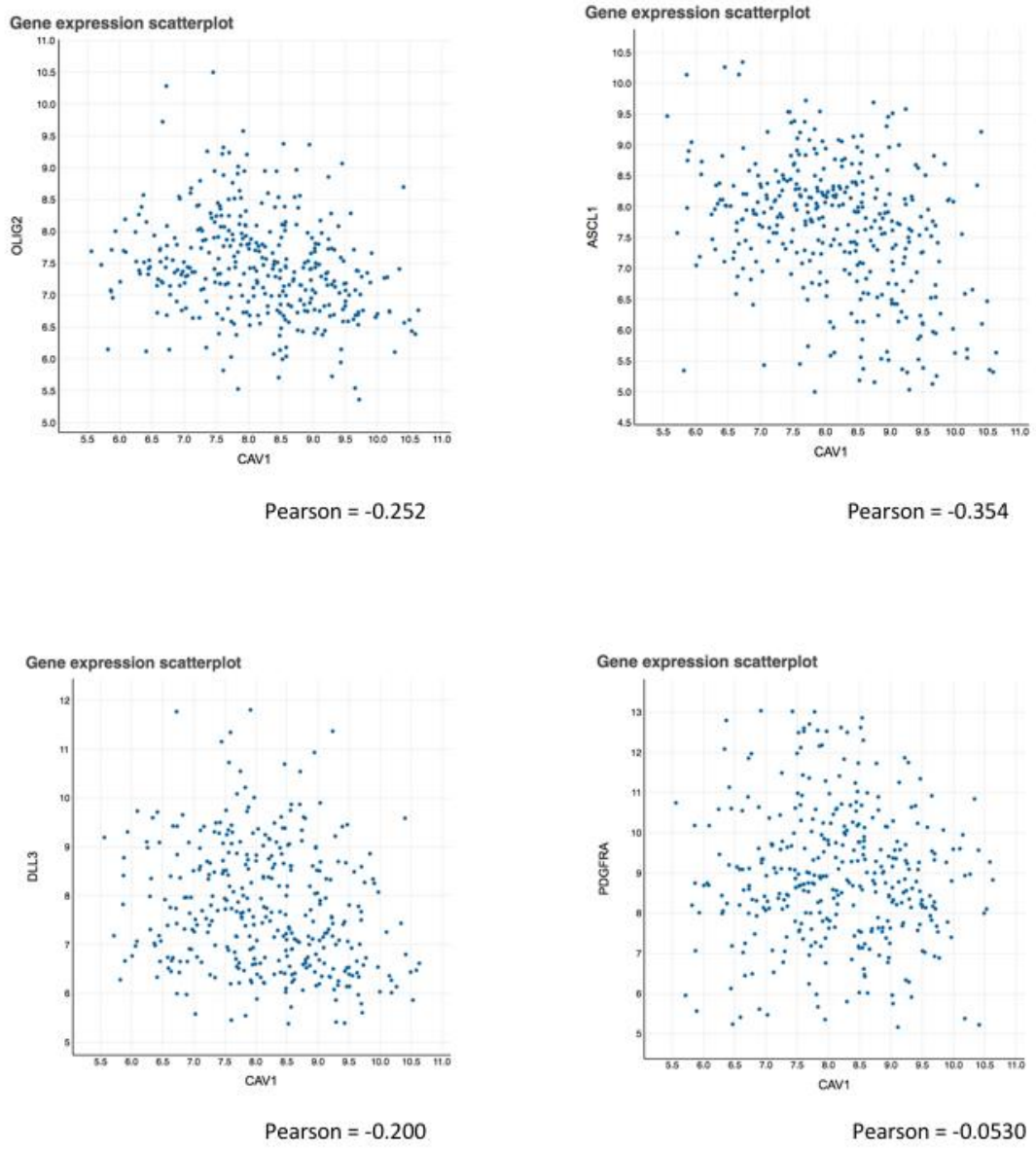

Fig. 13 GBM TCGA analysis of proneural markers and correlation with Cav-1 expression. Pearson correlation coefficient is indicated.

4.2 Assessment of Cav-1 expression under normoxia and hypoxia

Cav-1 expression was evaluated in a panel of GBM cell lines including GG14, BG7, BG5, GG16 and S24 under normoxic and hypoxic conditions. We observed that Cav-1 is strongly upregulated in GG14 and BG7 cell lines in hypoxia compared to normoxia. In contrast, S24 showed higher levels of Cav-1 in normoxia compared to hypoxia. There was no difference in cav-1 expression in GG16 and BG5 cells.

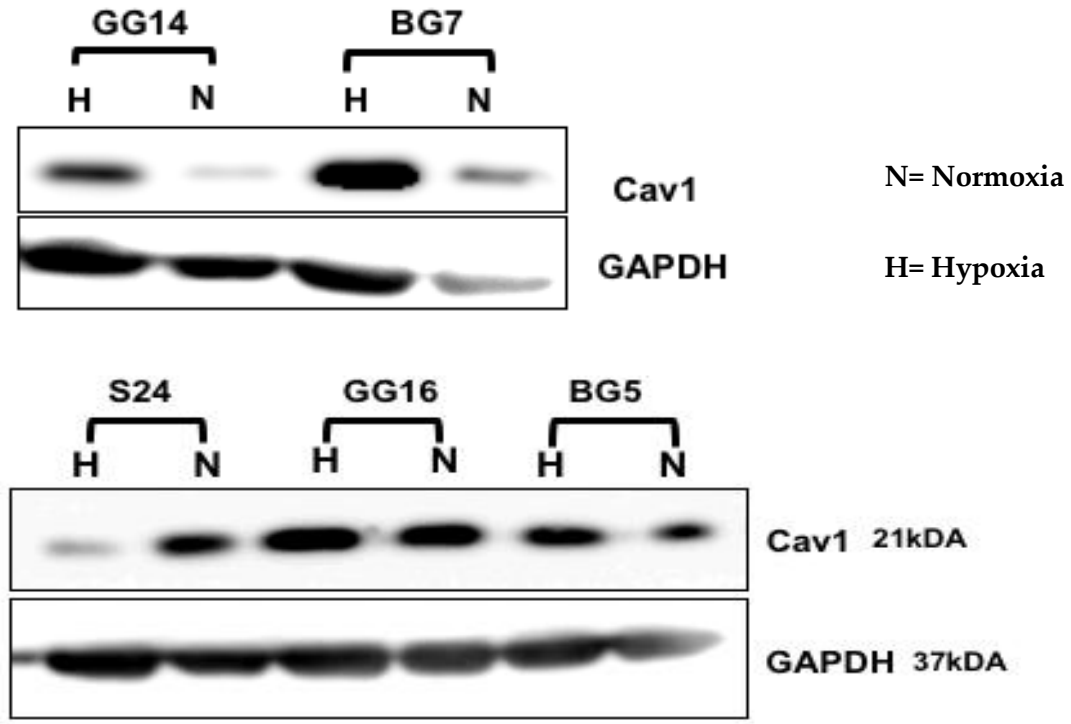

Fig. 14 Cav-1 expression under normoxic and hypoxic conditions in different human GBM cell lines. Western blot for Cav-1. GAPDH was used as a control.

4.3 Heterogeneity of Cav1 expression in GBM patient samples

To confirm our results from the cell lines, we performed immunohistochemistry staining in different human GBM tissue samples. Cav-1 is clearly upregulated around necrotic areas (hypoxic) areas in GBMs of patient 1, 2, and 5, while in patient 3, 4, and 6, Cav-1 expression is restricted to blood vessels (Fig. 15).

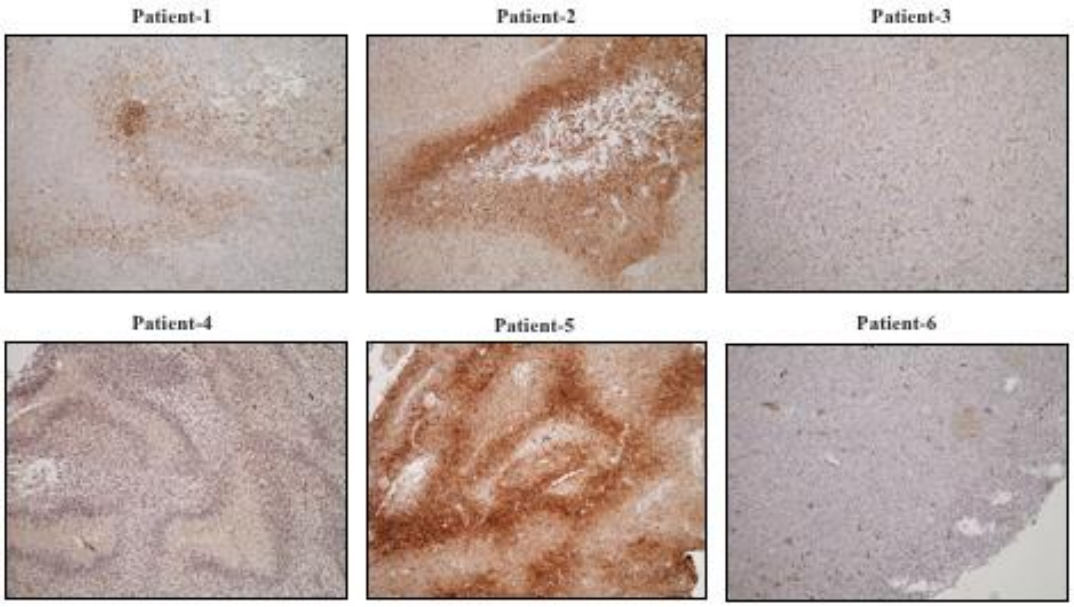

Fig. 15 Expression pattern of Cav-1 in human GBM patient samples. Xenograft tumor tissues derived from GBM human cell lines from different human patient samples. Representative Cav-1 IHC staining from a tissue showing Caveolin-1 is clearly upregulated in GBM patient sample 1, 2 and 5, while Cav-1 expression is restricted to blood vessels in patient 3, 4 and 6 respectively.

4.4 Induction of HIF-1α under hypoxia

To verify that GBM cell lines upregulate HIF-1α under hypoxia (1% O_2 for 72 hours), we performed western blot for HIF-1α under nomoxic and hypoxic conditions for BG5, GG16 and S24 cell lines (Fig. 16). In all 3 cell lines HIF-1α was upregulated under hypoxia compared to normoxia.

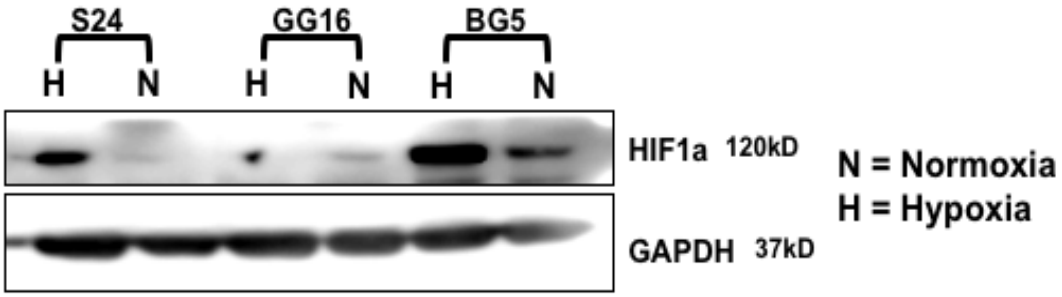

Fig. 16 Hypoxia induces upregulation of HIF-1α in GBM cell lines. Western blot for HIF-1α. GAPDH was used as a control.

4.5 Nuclear translocation of HIF-1α under hypoxia can be blocked by Digoxin

To investigate, if the HIF-1α inhibitor digoxin, a cardiac glycoside, could block the nuclear localization of HIF-1α, BG7 cells were examined under normoxia and hypoxia with or without digoxin by immunofluorescence. Digoxin is known to have modest effects on global protein synthesis but very potently inhibit HIF-1α mRNA translation.[99] A concentration of 150 nM Digoxin, which has been published previously to be effective (concentration, was added 1 hr prior to placing the BG7 cells under hypoxia for 18 hrs. Our Immunofluorescence data showed that the hypoxia-enhanced nuclear translocation of HIF-1α was slightly inhibited by digoxin (150 nM) compared to hypoxia without digoxin.

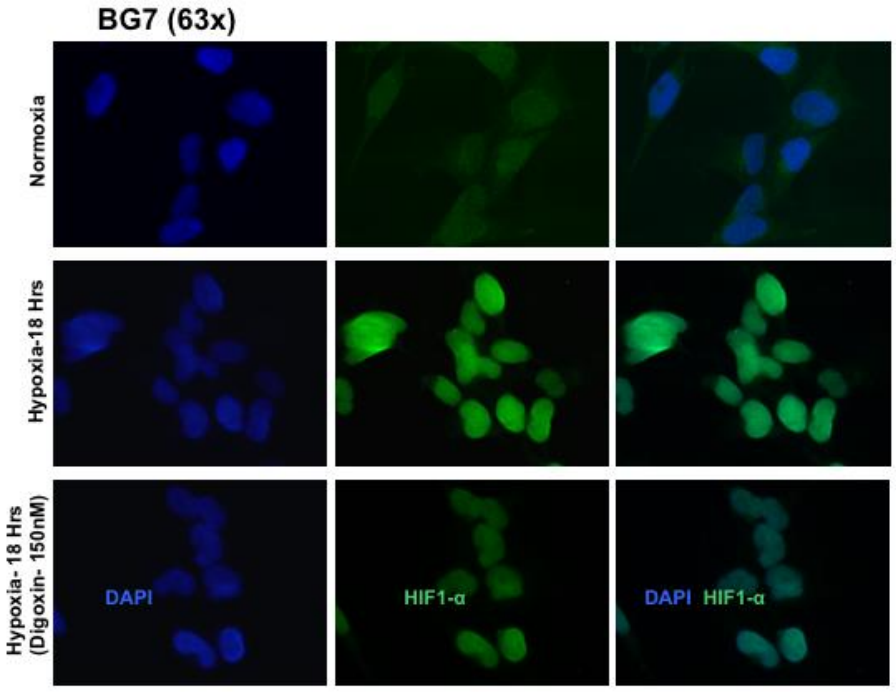

Fig. 17 All the representative images were acquired after 18 hours of incubation of the cells with drugs and control at 63x magnification. Staining was visualized by DAPI for hypoxic condition. Here we found, under hypoxic condition with 18hrs time period, digoxin (150nM concentration) could block the nuclear traslocation of HIF-1α but not completely and under normoxic conditions little or no nuclear expression of these transcription factors was detected.

4.6 Hypoxia induces a downregulation of proneural markers in GBM cells

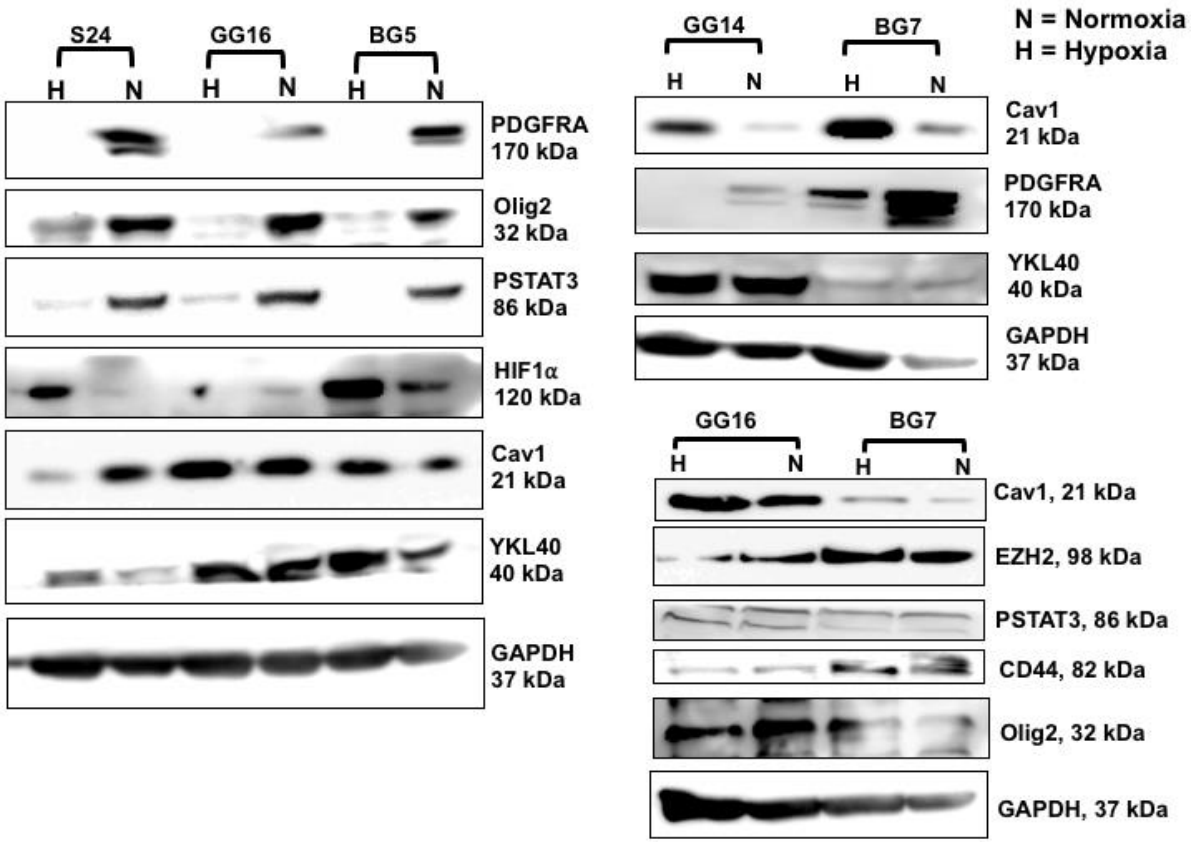

Fig. 18 Western blot analysis of different mesenchymal and proneural markers under normoxic and hypoxic conditions.

To explore whether hypoxia induced a proneural to mesenchymal transition in parallel to the upregulation of Cav-1, we performed western blot analyses from lysates of 5 different GBM cell lines for YKL40, pSTAT3, CD44 as representative mesenchymal markers along with proneural markers such as PDGFRA, Olig2 and EZH2 under normoxic and hypoxic conditions (1% O_2) for 72 hours. The proneural markers olig2 and PDGFRA were downregulated under hypoxic compared to normoxic conditions in all cell lines. The mesenchymal markers YKL40, CD44, pSTAT3 and EZH2 did not show such uniform pattern across the cell lines. Although YKL40 was upregulated in BG5 and S24 under hypoxia, Cav-1 was not upregulated in these cell lines under hypoxia. In S24, Cav-1 was even

downregulated under hypoxia. pSTAT3 was downregulated in BG5, GG16 and S24 under hypoxia while it did not show any change in BG7 and GG16. EZH2 and CD44 did not show substantial regulation either.

5. Discussion

The Cancer Genome Atlas Research Network (TCGA) first studied systematically Glioblastoma (GBM). The early publication from them in 2008 presented the results of genomic and transcriptomic analysis of 206 GBMs, including mutation sequencing of 600 genes in 91 samples.[100]

To study glioblastoma, several research groups are working on high dimensional gene profiling studies. For instance, studies examining copy number alterations[101] and gene expression profiling studies which identify gene signatures associated with EGFR overexpression, clinical features, and survival[102-104]

The advancements in genomic sequencing and transcriptome analysis have classified GBM into different molecular subtypes such as i) proneural, ii) classical iii) mesenchymal and iv) neural subtypes. These subtype names were chosen based on prior naming and the expression of signature genes.[105] The studies have established that overexpression of a mesenchymal gene expression signature (MGES) and loss of a proneural gene expression signature (PNGES) co-segregate with the poor prognosis group of glioma patients.[106]

A mesenchymal phenotype in GBM has been associated with tumour aggressiveness and elevated invasive potential. Interestingly, high levels of tumour necrosis were observed in tumours of patients having a mesenchymal subtype.[107]

A recent study proposed categorization of HIF regulated genes into those involving transcription factors, chromatin modifiers, enzymes, receptors, small GTPases, transporters adhesion molecules, surface molecules, membrane proteins, and miRs. Moreover, these genes have been shown to play a key role in the process of EMT and tumor metastasis. Hypoxic regions are frequently found in GBM and the presence of extensive hypoxic areas has been associated with worse prognosis in GBM patients, which has been linked to hypoxic cancer cells displaying a more malignant phenotype and being more resistant to chemotherapy and radiation.[108] The HIF transcription factors are instrumental for orchestrating adaptive responses to cope with oxygen shortage, and particularly HIF-1α is key in inducing expression of glycolytic enzymes and several angiogenic growth factors.[109] HIF-1α was found

to be upregulated in many of the malignant tumours primarily by hypoxia-mediated protein stabilization.[110]

In our study, we verified that HIF-1α was upregulated in primary GBM cell lines under hypoxia. Secondly, we observed that the hypoxia-induced expression of HIF-1α was suppressed by digoxin. Our immunoflurescence results demonstrated that under hypoxic conditions HIF-1α nuclear translocation was markedly inhibited by digoxin (150 nM) compared to hypoxia without digoxin. These data indicate that digoxin is a potent HIF-1α inhibitor which can reduce nuclear translocation of HIF-1α in BG7 cells. Immunofluorescence analysis highlighted HIF-1α immuno-reactivity predominantly in the nucleus based on DAPI counterstaining. However, the mechanisms of HIF-1α regulation remain unclear. Thus, future work needed to better understand the signalling pathways in HIF-1α regulation caused by cardiac glycosides (digoxin) under hypoxic conditions. Our results are consistent with some extent to the reported one. [111]

In GBM, HIF-1α seems to be primarily localized to the pseudopalisading cells around necrotic cores and to tumour cells at the invasive edge of the tumour that infiltrate the normal brain tissue [36]. Extensive necrosis and elevated levels of HIF-regulated genes are features that were more frequently found in mesenchymal GBM when compared to proneural GBM.[106] Despite the association between hypoxia and mesenchymal GBM, the potential molecular mediators that induce a mesenchymal shift are not fully characterized. In our study, we showed that proneural markers were downregulated under hypoxia across the cell lines while the regulation pattern for mesenchymal markers was more complex. Interestingly, overall, there was no clear upregulation of mesenchymal markers under hypoxia.

In our report, we found Cav-1 might be upregulated in GBM of the mesenchymal subtypes by the analysis of GBM TCGA data using the online tool “betastasis.com”. The data showed a correlation of Cav-1 expression with mesenchymal markers CEBPB, CD44, CHI3L1 (YKL40) and STAT3 and in contrast, analysis of proneural markers olig2, DLL3, ASCL1 and PDGFRA showed anti-correlation with Cav-1 expression.

Recent studies revealed that Caveolin-1 (Cav-1) is a critical regulator of tumor progression in a variety of cancers including glioblastoma multiforme where it has been implicated as either

a tumor suppressor or tumor promoter. Quann et al. showed significant upregulation of Cav-1 where genes are responsible for negative regulation of signal transduction, particularly within ERK, PI3K/AKT and mTOR pathways.[112] They also suggested that it has the capability to separate PI3K and mTOR activity. They also showed that ERK, PI3K and mTOR signaling axes are frequently upregulated in GBM. This suggests that loss of Cav-1 could lead to unchecked activation of these pathways.

In another report,[113] Cav-1 was able to affect the TGFβ pathway in glioblastoma cells. In U87MG cells, depletion of Cav-1 was associated with an increased secretion of TGFβ1, an increased expression of TGF-βRI and an increased phosphorylation of Smad2. Opposite effects were observed when caveolin-1 was overexpressed. They suggested that Cav-1 controls the secretion of TGFβ, the expression of TGFβRI and the activation status of Smad2 in U87MG cells.

Bailey and Liu also found that Cav-1 is up-regulated following induction of EMT.[114] Their results revealed that cells elongate and start to scatter prior to the up-regulation of Cav-1, suggesting that changes in Cav-1 expression may be a product of EMT.

Recently, Talasila et al. showed that Cav-1 is one of the top genes upregulated in the mesenchymal subtypes by gene expression data. Similarly, in our study, we observed that Cav-1 is strongly upregulated in GG14 and BG7 cell lines in hypoxia compared to normoxia. In contrast, S24 showed higher levels of Cav-1 in normoxia compared to hypoxia. There was no difference in Cav-1 expression in GBM cell lines including GG16 and BG5. This shows that Cav-1 expression and regulation can be very heterogenous between different GBM samples. We observed the same heterogeneity in tissue from patient samples, where Cav-1 was upregulated in hypoxic areas, however, not in all patient samples analysed. Future studies need to be performed to show if there is any correlation to specific mutations regarding the difference in Cav-1 expression.

Tissue hypoxia is caused by insufficient oxygen delivery, leading to activation of hypoxia-inducible factor (HIF). A wide range of HIF target genes was critical in the control of metabolism, cell proliferation, cell survival, angiogenesis, and iron uptake.[115] Hypoxia and necrosis both play key roles in tumor progression and resistance to treatment. However, *in*

vivo tumor growth is also characterized by the presence of ischemic and necrotic areas generated by oxygenation gradients and differential access to nutrients.[116] In our report, we performed IHC staining with several GBM tissue samples which were taken from 6 different patients to investigate the upregulation of Cav-1. We found from our investigation that Cav-1 is clearly upregulated in 3 GBM patient samples. In contrast, Cav-1 expression is restricted to blood vessels in other 3 patient samples.

Chiu et al. showed the relationship between pSTAT3 and Cav-1 and their clinical significance in human breast cancer brain metastasis.[117] They analysed several human breast cancer brain metastases samples which strongly suggested that activated STAT3 can binds directly to the Cav-1 promoter and inhibit its transcription. On the other hand, it was also showed that Cav-1 negatively regulates activation of STAT3 and invasion of brain-metastatic cancer cells. However, suppression of STAT3 activation inhibited the invasion and brain metastases of breast cancer cells in animal model. In our investigation, we found that pSTAT3 was downregulated in GBM cell lines including BG5, GG16 and S24 under hypoxia while it did not show any change in BG7 and GG16 cells.

The overlap of multiple hypoxia and mesenchymal signalling molecules and their integral role in the regulation of CSCs and the tumour microenvironment in GBM suggest the importance of understanding these mechanisms in designing future targeted therapies. Current evidence supports a mesenchymal subtype of GBM, which can evolve from other subtypes and portends a poorer clinical prognosis. Moreover, hypoxia and mesenchymal transformation involve multiple potentially targetable pathways and molecules.[59] The mesenchymal subclass has been associated with increased hypoxia and worse outcome. We have previously shown that HIF-1α is a central regulator of the genes upregulated in the angiogenic/mesenchymal tumors of our mode.

6. References

1. Chial, H. Genetic regulation of cancer. *Nature Education* **1** (2008).
2. http://www.who.int/en/news-room/fact-sheets/detail/cancer
3. Ahmedin, J. *et al.* Global cancer statistics. *CA: A Cancer Journal for Clinicians* **61**, 69-90 (2011).
4. Jacques, F. *et al.* Cancer incidence and mortality worldwide: Sources, methods and major patterns in GLOBOCAN 2012. *International Journal of Cancer* **136**, E359-E386 (2015).
5. Lengauer, C., Kinzler, K.W. & Vogelstein, B. Genetic instabilities in human cancers. *Nature* **396**, 643 (1998).
6. Hanahan, D. & Weinberg, Robert A. Hallmarks of Cancer: The Next Generation. *Cell* **144**, 646-674 (2011).
7. Pavlova, Natalya N. & Thompson, Craig B. The Emerging Hallmarks of Cancer Metabolism. *Cell Metabolism* **23**, 27-47 (2016).
8. Pecorino, L. *Molecular biology of cancer : mechanisms, targets, and therapeutics*, Edn. Fourth edition. (Oxford University Press, Oxford, United Kingdom; 2016).
9. Muller, P.A.J., Vousden, K.H. & Norman, J.C. p53 and its mutants in tumor cell migration and invasion. *The Journal of Cell Biology* **192**, 209 (2011).
10. Steeg, P.S. Tumor metastasis: mechanistic insights and clinical challenges. *Nature Medicine* **12**, 895 (2006).
11. Ribatti, D., Mangialardi, G. & Vacca, A. Stephen Paget and the 'seed and soil' theory of metastatic dissemination. *Clinical and Experimental Medicine* **6**, 145-149 (2006).
12. Ohgaki, H. & Kleihues, P. Population-based studies on incidence, survival rates, and genetic alterations in astrocytic and oligodendroglial gliomas. *J Neuropathol Exp Neurol* **64**, 479-489 (2005).
13. Louis, D.N. *et al.* The 2007 WHO Classification of Tumours of the Central Nervous System. *Acta Neuropathologica* **114**, 97-109 (2007).
14. Ostrom, Q.T. *et al.* CBTRUS Statistical Report: Primary Brain and Central Nervous System Tumors Diagnosed in the United States in 2008-2012. *Neuro Oncol* **17 Suppl 4**, iv1-iv62 (2015).
15. Stupp, R. *et al.* Radiotherapy plus Concomitant and Adjuvant Temozolomide for Glioblastoma. *New England Journal of Medicine* **352**, 987-996 (2005).
16. Friedmann-Morvinski, D. *et al.* Targeting NF-κB in glioblastoma: A therapeutic approach. *Science Advances* **2** (2016).
17. Kupp, R. *et al.* Lineage-Restricted OLIG2-RTK Signaling Governs the Molecular Subtype of Glioma Stem-like Cells. *Cell Reports* **16**, 2838-2845 (2016).
18. Wen, P.Y. & Kesari, S. Malignant Gliomas in Adults. *New England Journal of Medicine* **359**, 492-507 (2008).
19. Earle, K.M. The proper nomenclature for glioblastoma multiforme. *Int J Radiat Oncol Biol Phys* **1**, 805-808 (1976).

20. Panjabi, M.M., Dicker, D.B. & Dohrmann, G.J. Biomechanical quantification of experimental spinal cord trauma. *Journal of Biomechanics* **10**, 681-687 (1977).
21. Iacob, G. & Dinca, E.B. Current data and strategy in glioblastoma multiforme. *J Med Life* **2**, 386-393 (2009).
22. Zhen, L., Yufeng, C., Zhenyu, S. & Lei, X. Multiple extracranial metastases from secondary glioblastoma multiforme: a case report and review of the literature. *Journal of Neuro-Oncology* **97**, 451-457 (2010).
23. Moorthy, R.K. & Rajshekhar, V. Development of glioblastoma multiforme following traumatic cerebral contusion: case report and review of literature. *Surgical Neurology* **61**, 180-184 (2004).
24. Cobbs, C.S. Evolving evidence implicates cytomegalovirus as a promoter of malignant glioma pathogenesis. *Herpesviridae* **2**, 10 (2011).
25. Cobbs, C.S. *et al.* Human Cytomegalovirus Infection and Expression in Human Malignant Glioma. *Cancer Research* **62**, 3347 (2002).
26. Spinelli, V. *et al.* Occupational and environmental risk factors for brain cancer: a pilot case-control study in France. *La Presse Médicale* **39**, e35-e44 (2010).
27. Urbańska, K., Sokołowska, J., Szmidt, M. & Sysa, P. Glioblastoma multiforme – an overview. *Contemporary Oncology/Współczesna Onkologia* **18**, 307-312 (2014).
28. Wrensch, M., Minn, Y., Chew, T., Bondy, M. & Berger, M.S. Epidemiology of primary brain tumors: current concepts and review of the literature. *Neuro Oncol* **4**, 278-299 (2002).
29. Evans, S.M. *et al.* Hypoxia Is Important in the Biology and Aggression of Human Glial Brain Tumors. *Clinical Cancer Research* **10**, 8177 (2004).
30. Cooper, L.A.D. *et al.* The Tumor Microenvironment Strongly Impacts Master Transcriptional Regulators and Gene Expression Class of Glioblastoma. *The American Journal of Pathology* **180**, 2108-2119 (2012).
31. Brat, D.J. *et al.* Pseudopalisades in Glioblastoma Are Hypoxic, Express Extracellular Matrix Proteases, and Are Formed by an Actively Migrating Cell Population. *Cancer Research* **64**, 920 (2004).
32. Teicher, B.A. Hypoxia and drug resistance. *Cancer and Metastasis Reviews* **13**, 139-168 (1994).
33. Ohgaki, H. Epidemiology of Brain Tumors, in *Cancer Epidemiology: Modifiable Factors*. (ed. M. Verma) 323-342 (Humana Press, Totowa, NJ; 2009).
34. Kabat, G.C., Etgen, A.M. & Rohan, T.E. Do Steroid Hormones Play a Role in the Etiology of Glioma *Cancer Epidemiology Biomarkers & Prevention* **19**, 2421 (2010).
35. Tso, C.-L. *et al.* Distinct Transcription Profiles of Primary and Secondary Glioblastoma Subgroups. *Cancer Research* **66**, 159 (2006).
36. Ladha, J. *et al.* Glioblastoma-Specific Protein Interaction Network Identifies PP1A and CSK21 as Connecting Molecules between Cell Cycle–Associated Genes. *Cancer Research* **70**, 6437 (2010).

37. Phillips, H.S. *et al.* Molecular subclasses of high-grade glioma predict prognosis, delineate a pattern of disease progression, and resemble stages in neurogenesis. *Cancer Cell* **9**, 157-173 (2006).
38. Louis, D.N. *et al.* The 2016 World Health Organization Classification of Tumors of the Central Nervous System: a summary. *Acta Neuropathologica* **131**, 803-820 (2016).
39. Hiroko, O. & Paul, K. Genetic alterations and signaling pathways in the evolution of gliomas. *Cancer Science* **100**, 2235-2241 (2009).
40. Oberndorfer, S. *et al.* The End-of-Life Hospital Setting in Patients with Glioblastoma. *Journal of Palliative Medicine* **11**, 26-30 (2008).
41. Sizoo, E.M. *et al.* Symptoms and problems in the end-of-life phase of high-grade glioma patients. *Neuro Oncol* **12**, 1162-1166 (2010).
42. Lakhan, S.E. & Harle, L. Difficult diagnosis of brainstem glioblastoma multiforme in a woman: a case report and review of the literature. *Journal of Medical Case Reports* **3**, 87 (2009).
43. Larjavaara, S. *et al.* Incidence of gliomas by anatomic location. *Neuro Oncol* **9**, 319-325 (2007).
44. Drevelegas, A. *Imaging of Brain Tumors with Histological Correlations*, Edn. 2 nd. (Springer-Verlag, Berlin Heidelberg; 2011).
45. Kleihues, P., Cavenee, W.K. & International Agency for Research on Cancer. *Pathology and genetics of tumours of the nervous system*. (IARC Press, Lyon; 2000).
46. Puli, S., Lai, J.C.K. & Bhushan, A. Inhibition of matrix degrading enzymes and invasion in human glioblastoma (U87MG) Cells by isoflavones. *Journal of Neuro-Oncology* **79**, 135-142 (2006).
47. Kesari, S. Understanding Glioblastoma Tumor Biology: The Potential to Improve Current Diagnosis and Treatments. *Seminars in Oncology* **38**, S2-S10 (2011).
48. Mammoto, T. *et al.* Role of Collagen Matrix in Tumor Angiogenesis and Glioblastoma Multiforme Progression. *The American Journal of Pathology* **183**, 1293-1305 (2013).
49. Codrici, E., Enciu, A.-M., Popescu, I.-D., Mihai, S. & Tanase, C. Glioma Stem Cells and Their Microenvironments: Providers of Challenging Therapeutic Targets. *Stem Cells International* **2016**, 20 (2016).
50. Hu, M. & Polyak, K. Microenvironmental regulation of cancer development. *Current Opinion in Genetics & Development* **18**, 27-34 (2008).
51. Chen, J.L.-Y. *et al.* The Genomic Analysis of Lactic Acidosis and Acidosis Response in Human Cancers. *PLOS Genetics* **4**, e1000293 (2008).
52. Bar, E.E., Lin, A., Mahairaki, V., Matsui, W. & Eberhart, C.G. Hypoxia Increases the Expression of Stem-Cell Markers and Promotes Clonogenicity in Glioblastoma Neurospheres. *The American Journal of Pathology* **177**, 1491-1502 (2010).
53. Thambi, T., Park, J.H. & Lee, D.S. Hypoxia-responsive nanocarriers for cancer imaging and therapy: recent approaches and future perspectives. *Chemical Communications* **52**, 8492-8500 (2016).

54. Wan, J.U.N., Wu, W.E.I. & Zhang, R. Local recurrence of small cell lung cancer following radiofrequency ablation is induced by HIF-1α expression in the transition zone. *Oncology Reports* **35**, 1297-1308 (2016).
55. Tonissi, F. *et al.* Reoxygenation Reverses Hypoxia-related Radioresistance in Head and Neck Cancer Cell Lines. *Anticancer Res* **36**, 2211-2215 (2016).
56. Semenza, G.L. Oxygen Sensing, Hypoxia-Inducible Factors, and Disease Pathophysiology. *Annual Review of Pathology: Mechanisms of Disease* **9**, 47-71 (2014).
57. Wenger, R.H., Stiehl, D.P. & Camenisch, G. Integration of Oxygen Signaling at the Consensus HRE. *Science's STKE* **2005**, re12 (2005).
58. Colwell, N. *et al.* Hypoxia in the glioblastoma microenvironment: shaping the phenotype of cancer stem-like cells. *Neuro Oncol* **19**, 887-896 (2017).
59. Karsy, M., Guan, J., Jensen, R., Huang, L.E. & Colman, H. The Impact of Hypoxia and Mesenchymal Transition on Glioblastoma Pathogenesis and Cancer Stem Cells Regulation. *World Neurosurgery* **88**, 222-236 (2016).
60. Rong, Y., Durden, D.L., Van Meir, E.G. & Brat, D.J. 'Pseudopalisading' necrosis in glioblastoma: a familiar morphologic feature that links vascular pathology, hypoxia, and angiogenesis. *J Neuropathol Exp Neurol* **65**, 529-539 (2006).
61. Kahlert, U.D. *et al.* Activation of canonical WNT/β-catenin signaling enhances in vitro motility of glioblastoma cells by activation of ZEB1 and other activators of epithelial-to-mesenchymal transition. *Cancer Letters* **325**, 42-53 (2012).
62. Kahlert, U.D., Nikkhah, G. & Maciaczyk, J. Epithelial-to-mesenchymal(-like) transition as a relevant molecular event in malignant gliomas. *Cancer Lett* **331**, 131-138 (2013).
63. Iwadate, Y. Epithelial-mesenchymal transition in glioblastoma progression. *Oncology Letters* **11**, 1615-1620 (2016).
64. Parat, M.-O. & Riggins, G.J. Caveolin-1, caveolae, and glioblastoma. *Neuro-Oncology* **14**, 679-688 (2012).
65. Tiwari, A. *et al.* Caveolin-1 is an aggresome-inducing protein. *Sci Rep* **6**, 38681 (2016).
66. Williams, T.M. & Lisanti, M.P. The Caveolin genes: from cell biology to medicine. *Annals of Medicine* **36**, 584-595 (2004).
67. Hill, M.M. *et al.* PTRF-Cavin, a Conserved Cytoplasmic Protein Required for Caveola Formation and Function. *Cell* **132**, 113-124 (2008).
68. Bastiani, M. *et al.* MURC/Cavin-4 and cavin family members form tissue-specific caveolar complexes. *The Journal of Cell Biology* **185**, 1259 (2009).
69. Salem, A.F. *et al.* Caveolin-1 promotes pancreatic cancer cell differentiation and restores membranous E-cadherin via suppression of the epithelial-mesenchymal transition. *Cell Cycle* **10**, 3692-3700 (2011).
70. Deurs, B.v., Roepstorff, K., Hommelgaard, A.M. & Sandvig, K. Caveolae: anchored, multifunctional platforms in the lipid ocean. *Trends in Cell Biology* **13**, 92-100 (2003).
71. Martin, S. *et al.* Caveolin-1 regulates glioblastoma aggressiveness through the control of α5β1 integrin expression and modulates glioblastoma

responsiveness to SJ749, an α5β1 integrin antagonist. *Biochimica et Biophysica Acta (BBA) - Molecular Cell Research* **1793**, 354-367 (2009).
72. Scherer, P.E., Williams, S., Fogliano, M., Baldini, G. & Lodish, H.F. A novel serum protein similar to C1q, produced exclusively in adipocytes. *J Biol Chem* **270**, 26746-26749 (1995).
73. Michel, V. & Bakovic, M. Lipid rafts in health and disease. *Biology of the Cell* **99**, 129-140 (2012).
74. Shatz, M. & Liscovitch, M. Caveolin-1: a tumor-promoting role in human cancer. *Int J Radiat Biol* **84**, 177-189 (2008).
75. Patel, H.H., Murray, F. & Insel, P.A. Caveolae as Organizers of Pharmacologically Relevant Signal Transduction Molecules. *Annual Review of Pharmacology and Toxicology* **48**, 359-391 (2008).
76. Gupta, R., Toufaily, C. & Annabi, B. Caveolin and cavin family members: Dual roles in cancer. *Biochimie* **107**, 188-202 (2014).
77. Chatterjee, M. *et al.* Caveolin-1 is Associated with Tumor Progression and Confers a Multi-Modality Resistance Phenotype in Pancreatic Cancer. *Scientific Reports* **5**, 10867 (2015).
78. Koleske, A.J., Baltimore, D. & Lisanti, M.P. Reduction of caveolin and caveolae in oncogenically transformed cells. *Proceedings of the National Academy of Sciences* **92**, 1381 (1995).
79. Galbiati, F. *et al.* Targeted downregulation of caveolin-1 is sufficient to drive cell transformation and hyperactivate the p42/44 MAP kinase cascade. *The EMBO Journal* **17**, 6633 (1998).
80. Sunaga, N. *et al.* Different Roles for Caveolin-1 in the Development of Non-Small Cell Lung Cancer versus Small Cell Lung Cancer. *Cancer Research* **64**, 4277 (2004).
81. Navarro, A., Anand-Apte, B. & Parat, M.-O. A role for caveolae in cell migration. *The FASEB Journal* **18**, 1801-1811 (2004).
82. Laflamme, M.A. *et al.* Formation of Human Myocardium in the Rat Heart from Human Embryonic Stem Cells. *The American Journal of Pathology* **167**, 663-671 (2005).
83. Schwarz, B.T. *et al.* LIGHT Signals Directly to Intestinal Epithelia to Cause Barrier Dysfunction via Cytoskeletal and Endocytic Mechanisms. *Gastroenterology* **132**, 2383-2394 (2007).
84. Song, L., Ge, S. & Pachter, J.S. Caveolin-1 regulates expression of junction-associated proteins in brain microvascular endothelial cells. *Blood* **109**, 1515 (2007).
85. Griffoni, C. *et al.* Knockdown of Caveolin-1 by Antisense Oligonucleotides Impairs Angiogenesis in Vitro and in Vivo. *Biochemical and Biophysical Research Communications* **276**, 756-761 (2000).
86. Beardsley, A. *et al.* Loss of caveolin-1 polarity impedes endothelial cell polarization and directional movement. *J Biol Chem* **280**, 3541-3547 (2005).
87. Holdhoff, M. *et al.* Use of personalized molecular biomarkers in the clinical care of adults with glioblastomas. *Journal of Neuro-Oncology* **110**, 279-285 (2012).

88. Rodriguez, O.C. *et al.* Dietary downregulation of mutant p53 levels via glucose restriction. *Cell Cycle* **11**, 4436-4446 (2012).
89. Sotgia, F. *et al.* Understanding the Warburg effect and the prognostic value of stromal caveolin-1 as a marker of a lethal tumor microenvironment. *Breast Cancer Research* **13**, 213 (2011).
90. Tanowitz, H.B., Machado, F.S. & Albanese, C. An expanded role for Caveolin-1 in brain tumors. *Cell Cycle* **12**, 1485-1486 (2013).
91. Ohgaki, H. & Kleihues, P. Genetic Pathways to Primary and Secondary Glioblastoma. *The American Journal of Pathology* **170**, 1445-1453 (2007).
92. Volonte, D. *et al.* Caveolin-1 promotes the tumor suppressor properties of oncogene-induced cellular senescence. *J Biol Chem* **293**, 1794-1809 (2018).
93. Jenkins, R.B. *et al.* A Molecular Cytogenetic Analysis of 7q31 in Prostate Cancer. *Cancer Research* **58**, 759 (1998).
94. Zenklusen, J.C., Thompson, J.C., Klein-Szanto, A.J.P. & Conti, C.J. Frequent Loss of Heterozygosity in Human Primary Squamous Cell and Colon Carcinomas at 7q31.1: Evidence for a Broad Range Tumor Suppressor Gene. *Cancer Research* **55**, 1347 (1995).
95. Zenklusen, J.C., Thompson, J.C., Troncoso, P., Kagan, J. & Conti, C.J. Loss of Heterozygosity in Human Primary Prostate Carcinomas: A Possible Tumor Suppressor Gene at 7q31.1. *Cancer Research* **54**, 6370 (1994).
96. Cohen, A.W., Hnasko, R., Schubert, W. & Lisanti, M.P. Role of Caveolae and Caveolins in Health and Disease. *Physiological Reviews* **84**, 1341-1379 (2004).
97. Tanowitz, H.B., Machado, F.S., Avantaggiati, M.L. & Albanese, C. An expanded role for Caveolin-1 in brain tumors. *Cell Cycle* **12**, 1485-1486 (2013).
98. Talasila, K.M. *et al.* The angiogenic switch leads to a metabolic shift in human glioblastoma. *Neuro-Oncology* **19**, 383-393 (2017).
99. Zhang, H. *et al.* Digoxin and other cardiac glycosides inhibit HIF-1α synthesis and block tumor growth. *Proceedings of the National Academy of Sciences* **105**, 19579 (2008).
100. Brennan, Cameron W. *et al.* The Somatic Genomic Landscape of Glioblastoma. *Cell* **155**, 462-477 (2013).
101. Beroukhim, R. *et al.* Assessing the significance of chromosomal aberrations in cancer: Methodology and application to glioma. *Proceedings of the National Academy of Sciences* **104**, 20007 (2007).
102. Freije, W.A. *et al.* Gene Expression Profiling of Gliomas Strongly Predicts Survival. *Cancer Research* **64**, 6503 (2004).
103. Liang, Y. *et al.* Gene expression profiling reveals molecularly and clinically distinct subtypes of glioblastoma multiforme. *Proceedings of the National Academy of Sciences of the United States of America* **102**, 5814 (2005).
104. Mischel, P.S. *et al.* Identification of molecular subtypes of glioblastoma by gene expression profiling. *Oncogene* **22**, 2361 (2003).
105. Hodgson, J.G. *et al.* Comparative analyses of gene copy number and mRNA expression in glioblastoma multiforme tumors and xenografts. *Neuro Oncol* **11**, 477-487 (2009).

106. Carro, M.S. *et al.* The transcriptional network for mesenchymal transformation of brain tumours. *Nature* **463**, 318 (2009).
107. Verhaak, R.G.W. *et al.* Integrated Genomic Analysis Identifies Clinically Relevant Subtypes of Glioblastoma Characterized by Abnormalities in PDGFRA, IDH1, EGFR, and NF1. *Cancer Cell* **17**, 98-110 (2010).
108. Hsieh, C.H. *et al.* NADPH oxidase subunit 4-mediated reactive oxygen species contribute to cycling hypoxia-promoted tumor progression in glioblastoma multiforme. *PLoS One* **6**, e23945 (2011).
109. Carmeliet, P. & Jain, R.K. Principles and mechanisms of vessel normalization for cancer and other angiogenic diseases. *Nat Rev Drug Discov* **10**, 417-427 (2011).
110. Semenza, G.L. Intratumoral hypoxia, radiation resistance, and HIF-1. *Cancer Cell* **5**, 405-406 (2004).
111. Wei, D. *et al.* Digoxin downregulates NDRG1 and VEGF through the inhibition of HIF-1alpha under hypoxic conditions in human lung adenocarcinoma A549 cells. *Int J Mol Sci* **14**, 7273-7285 (2013).
112. Quann, K. *et al.* Caveolin-1 is a negative regulator of tumor growth in glioblastoma and modulates chemosensitivity to temozolomide. *Cell Cycle* **12**, 1510-1520 (2013).
113. C., C.E. *et al.* Involvement of the TGFβ pathway in the regulation of α5β1 integrins by caveolin-1 in human glioblastoma. *International Journal of Cancer* **131**, 601-611 (2012).
114. Bailey, K.M. & Liu, J. Caveolin-1 up-regulation during epithelial to mesenchymal transition is mediated by focal adhesion kinase. *J Biol Chem* **283**, 13714-13724 (2008).
115. Xie, L. *et al.* Hypoxia-inducible factor/MAZ-dependent induction of caveolin-1 regulates colon permeability through suppression of occludin, leading to hypoxia-induced inflammation. *Mol Cell Biol* **34**, 3013-3023 (2014).
116. Daster, S. *et al.* Induction of hypoxia and necrosis in multicellular tumor spheroids is associated with resistance to chemotherapy treatment. *Oncotarget* **8**, 1725-1736 (2017).
117. Chiu, W.T. *et al.* Caveolin-1 upregulation mediates suppression of primary breast tumor growth and brain metastases by stat3 inhibition. *Cancer Res* **71**, 4932-4943 (2011).